CONTRACT REPORT NO. OST85-00423

CIRCULATING FLUIDIZED BED COMBUSTION OF COAL, WOODWASTES AND PITCH

J.R. Grace and C.J. Lim
Department of Chemical Engineering and Pulp and Paper Centre
The University of British Columbia
Vancouver, Canada V6T 1W5

Final Report, Prepared for Energy, Mines and Resources Canada
Under Contract 24St.23440-6-9007

MICROFICHE

December, 1987.

77 pp

CIRCULATING FLUIDIZED BED COMBUSTION OF COAL, WOODWASTES AND PITCH

Final Report

by J.R. Grace and C.J. Lim

Department of Chemical Engineering and

Pulp and Paper Centre,

University of British Columbia,
Vancouver, Canada V6T 1W5.

Work on this project was conducted under the auspices of the Canada Centre for Mineral and Energy Technology, Energy, Mines and Resources Canada.

DSS File Number: 24ST.23440-6-9007

DSS Contract Serial Number: OST85-00423

CANMET Scientific Authority: Dr. E.J. Anthony

December, 1987

ABSTRACT

A pilot scale circulating fluidized bed combustor of cross-sectional area 152 mm x 152 mm and height 7.32 m was completed with the addition of feeding systems for solid and liquid fuels and analytical instruments for measuring the concentrations of key components in the off-gases. An L-valve is employed to return solids captured in a refractory-lined primary cyclone to the base of the riser. The amount of heat transfer cooling surface had to be reduced from the original design due to high heat losses from the combustion chamber and return circuit. With this change and careful attention to feeding in particular, trial burns of total duration 478 h were carried out with a number of coals, with two woodwaste materials (sawdust and hogfuel) and with two pitches originating from unconventional fuel upgrading processes. Limestone was used as a sorbent for the high sulphur coal and pitch materials. Stable combustion conditions were obtained with most of the fuels tested. Combustion efficiencies were generally in the 92-99 % range, somewhat lower on average than values reported in the literature, probably due to the limited height of the reactor and the fact that fines captured in the secondary cyclone were not recycled to the base of the riser.

With high sulphur Minto coal from New Brunswick, sulphur capture efficiencies of 72-88 % were achieved with Ca:S molar ratios of 1.36 to 2.7. NOx emissions were consistently 150 ppm or lower for the coal runs. Varying the secondary/primary air ratio, superficial gas velocity and solids circulation rate had relatively little influence on the combustion characteristics and gaseous emissions for the range of conditions investigated, conditions which are consistent with current industrial practice. Solids samples withdrawn from the bottom of the combustion chamber itself (bed drain), from the L-valve and from the secondary cyclone consistently showed levels of calcium sulphide less than 1 % by weight.

With the woodwaste materials, there was a tendency for heat release to occur higher in the unit and by further burning in the primary and secondary cyclones. NOx levels in the off-gases were always 100 ppm or lower for the two woodwaste materials tested, sawdust and hogfuel. Levels of CO and methane measured at the exit from the reactor assembly fluctuated wildly, these fluctuations probably originating from periodic delivery of plugs of solid feed material by the screw feeder. The heavier hogfuel generally gave smaller fluctuations and lower CO and methane emissions than the lighter sawdust material.

Some difficulties were encountered in the pitch combustion trials in feeding the materials in liquid form and in preventing agglomeration inside the combustion chamber. For the first pitch tested, obtained from the CANMET hydrocracking demonstration unit at the Petrocan refinery in Montreal East, these difficulties were overcome by maintaining the entire feed circuit at a minimum temperature of 190 C, while the second problem was solved by starting up the unit with coal and then switching over to pitch once the temperature in the entire circulating bed circuit was sufficiently high. NOx emissions for this pitch material were consistently less than 170 ppm while sulphur capture was 78 to 85 % for Ca:S molar ratios of 1.5 to 2.3. Preliminary results indicate that the vanadium present in the original pitch is not entirely captured in the solids, although there was no baghouse present during these trials so that it is possible that substantial capture may be achieved in the finest solid material.

Only partial success was achieved in burning a second pitch material supplied by AOSTRA and produced by the H-Oil process. Difficulties in this case were due to malfunctions in the building ventilation system. The results which were achieved for this case did, however, appear to be consistent with those for the CANMET pitch.

Temperature profiles obtained under combustion conditions showed temperatures to be quite uniform around the entire circuit with maximum variations of the order of 30 C for coal and somewhat higher for the woodwaste materials in particular. Heat transfer measurements were obtained both with membrane wall cooling surfaces and with a single vertical tube at different radial positions. The length of the cooling surface was shown to be important, so that miniature heat transfer probes can give misleading results. Radiation typically accounts for an increase in the heat transfer coefficient of the order of 60-80 W/m2K for temperatures in the usual combustion range, i.e. 850-900 C. Heat transfer coefficients depend strongly on the density of the suspension of particles but only weakly on the superficial gas velocity and particle size for the conditions studied.

ACKNOWLEDGEMENT

A project of this scope and complexity could not have been carried out without the active participation and cooperation of many people.

We are especially indebted to the graduate students and research personnel who so willingly and cheerfully worked at all times of the night and day, often under adverse conditions. In alphabetical order they were Hugh Ackroyd, Clive Brereton, Jamal Chaouki, Gordon Cheng, Dr. Robert Legros, Dr. Hongzhong Li, Andrea Townson, Wang Ningde, Richard Wu, Weimiao Yu, Jiansheng Zhao and Jesse Zhu. The assistance of Claude Desjardins at the design stage was also invaluable.

Analytical work related to the contract was carried out at U.B.C. by Dr. K.C. Teo, Roger Quon and Ken Vidal. We are grateful for their help. The Chemical Engineering Workshop under John Baranowski was always ready to lend a hand when needed, and we greatly appreciate their assistance. Dr. Richard Kerekes was responsible for our equipment being housed in the Pulp and Paper Centre, without which life would have been considerably more difficult. Ken Wong was helpful in a myriad of details concerning the Centre and its mechanical services.

We also must acknowledge assistance from a number of persons outside U.B.C. Foremost among these is Dr. E.J. Anthony of Energy, Mines and Resources in Ottawa, the Scientific Authority on the contract, who supported our work throughout with optimism and constructive suggestions. Others who were helpful include Geoff Ross of Environment Canada, Chris Doiron of New Brunswick Power, John Foong of Petrocan, and Roger Bailey of AOSTRA.

TABLE OF CONTENTS

ABSTRACT	i
ACKNOWLEDGEMENT	iii
LIST OF FIGURES	v
LIST OF TABLES	vii
1. INTRODUCTION	1
2. THE EXPERIMENTAL FACILITY	5
2.1 The Reactor	5
2.2 Air Supply and Preheating System	5
2.3 Solids Feed System	9
2.4 Liquid Feed System	11
2.5 Heat Transfer Surface	13
2.6 Solids Recycle System	13
2.7 Gas Exit and Analysis	17
2.8 Solids Sampling	17
2.9 Instrumentation and Data Acquisition	19
2.10 Properties of Fuels, Sorbents and Inert Particles	19
3. EXPERIMENTAL PROCEDURES AND PROBLEMS ENCOUNTERED	27
3.1 Start-up of the Unit	27
3.2 Solids Sampling Procedure	28
3.3 Problems Encountered	29
3.4 Shutdown of the Unit	30
4. HEAT TRANSFER AND TEMPERATURE PROFILES	31
4.1 Heat Transfer Coefficients	31
4.1.1 Membrane wall measurements	31
4.1.2 Single vertical tube measurements	38
4.2 Temperature Profiles	43
5. COMBUSTION TESTS	46
5.1 Overview	46
5.2 Minto Coal Tests	46
5.3 Woodwaste Combustion Tests	52
5.4 Pitch Combustion Tests	55
5.4.1 CANMET pitch combustion trials	56
5.4.2 AOSTRA H-Oil pitch combustion trials	60
6. CONCLUSIONS AND RECOMMENDATIONS	62
6.1 Conclusions	62
6.2 Recommendations	63
NOMENCLATURE	65
REFERENCES	66

LIST OF FIGURES

page

Figure 2.1: Simplified schematic diagram of experimental circulating fluidized bed combustion facility. 6

Figure 2.2: View of principal refractory-lined reaction chamber. 7

Figure 2.3: Distributor plate configuration. Solid and broken arrows refer to lower and upper holes respectively. All dimensions are in mm. 8

Figure 2.4: Secondary air inlet geometry. All dimensions are in mm. 8

Figure 2.5: Solid feed configurations: a) Dual hopper for coal and sorbent with control by rotary valves; b) Live bottom hopper for woodwastes; c) Pneumatic feeding for coal/sorbent mixtures. 1: Large hopper; 2: Cylindrical hopper; 3: Air; 4: Rotary valve; 5: Screw feeder; 6: Blind flange; 7: Reactor; 8: Coal; 9: Sorbent; 10: Woodwaste; 11: Coal/sorbent mixture. 10

Figure 2.6: Liquid feed configuration. 12

Figure 2.7: Nozzle for pitch feeding. 12

Figure 2.8: Membrane wall cooling surfaces: (a) plan view; (b) section view showing thermocouple positions. All dimensions are in mm. 14

Figure 2.9: Quartz window and calorimetric section for measuring solids circulation rate. All dimensions are in mm. 16

Figure 2.10: Gas sampling system. 18

Figure 2.11: Thermocouple locations in CFBC reactor system. 20

Figure 2.12: Pressure tap locations in CFBC reactor system. 21

Figure 4.1: Average suspension to membrane wall heat transfer coefficient for 188 um particles as a function of suspension density for different secondary/primary flow ratios. Open and closed symbols refer to the upper and lower exchange surfaces respectively. 32

Figure 4.2: Average suspension to membrane wall heat transfer coefficient for 356 um sand particles as a function of suspension density. Secondary/primary air ratio = 0 for all cases. Open and filled symbols refer to upper and lower heat transfer surfaces respectively. 33

Figure 4.3: Influence of superficial gas velocity on average suspension to membrane wall heat transfer coefficient at three different suspension densities for the 188 um sand. 35

Figure 4.4: Typical longitudinal profiles of heat transfer coefficient and suspension density for (a) upper surface, and (b) lower surface. Coefficients are obtained between thermocouples 1-3, 3-6, 6-8 in Figure 2.8(b) for 188 um sand particles. 37

Figure 4.5: Heat transfer coefficient for section of upper heat exchange surface between thermocouples 1 and 3 in Figure 2.8(b) for two sizes of sand. 39

Figure 4.6: Suspension to membrane wall heat transfer coefficients at combustion temperatures (750-850 C) for 303 um mean particle size and U = 6-10 m/s (shown by points), compared with lines obtained under low temperature conditions (150-400 C) where radiation is negligible. 40

Figure 4.7: Suspension to vertical tube heat transfer coefficients for elevated temperatures, U = 6-8 m/s and mean particle diameter 250-300 um. 41

Figure 4.8: Crossplot of suspension to vertical tube heat transfer coefficient vs temperature for three suspension densities. Conditions as for Figure 4.7. 42

Figure 4.9: Suspension to vertical tube heat transfer coefficients for four different lateral distances between the axis of the tube and the wall. Upper four curves: T = 854 C; U = 8.5 m/s; dp = 227 um. Lower four curves: T = 343 C; U = 6.0 m/s; dp = 299 um. 44

Figure 4.10: Typical temperature profile during combustion trial. Highvale coal; upper membrane cooling surface only in place. 45

Figure 5.1: Sulphur capture versus Ca:S molar ratio for Minto coal and CANMET pitch tests. 49

Figure 5.2: NOx emissions versus secondary/primary air ratio for four different fuels. Operating conditions are given in Tables 5.2 to 5.6. 49

Figure 5.3: Particle size distributions for particulate materials withdrawn at the end of the Minto coal tests. For operating conditions see Table 5.2. 51

Figure 5.4: Instantaneous temperature profile during sawdust combustion trial. 53

LIST OF TABLES

	page
Table 2.1: Proximate and Ultimate Analyses of Solid Fuels	22
Table 2.2: Properties of Pitch Materials Tested	23
Table 2.3: Physical Properties of Particulate Materials	24
Table 2.4: Chemical Analysis of Limestones and Inerts	25
Table 2.5: Ash Composition of Fuels	25
Table 2.6: Particle Size Distributions of Solid Feed Materials	26
Table 4.1: Particle Size Distributions of Sand Used During the Heat Transfer Experiments	34
Table 5.1: Chronology of Combustion Runs	47
Table 5.2: Test Results for Minto Coal/Elmtree Limestone for Different Calcium to Sulphur Ratios	48
Table 5.3: Effect of Operating Variable Changes on Emission Levels: Minto Coal/Elmtree Limestone; Ca:S = 1.36	48
Table 5.4: Superficial Gas Velocities, Secondary/Primary Air Ratios, and Temperatures for Sawdust and Hogfuel Burning	54
Table 5.5: Gaseous Emissions and Suspension Densities for Sawdust and Hogfuel Burning	54
Table 5.6: Summary of Combustion Results for CANMET Pitch	57
Table 5.7: Metals Content in Solid Samples from CANMET Pitch Trial	59
Table 5.8: Summary of Combustion Results for H-Oil Pitch	61

1. INTRODUCTION

Circulating fluidized bed combustion (CFBC) has attracted considerable attention during the past decade. CFB boilers are now capturing a significant fraction of the market for industrial and utility scale boilers. At the same time, there is widespread interest in applications of circulating bed boilers for combustion of a wide variety of unusual fuels and waste materials.

Circulating fluidized beds differ from conventional (bubbling) fluidized beds in having higher superficial gas velocities (typically 5-10 m/s as compared with 1-3 m/s) and higher overall voidages (typically 0.9 to 0.98 compared with 0.6 to 0.75). In addition, the particles are generally somewhat finer (typically 50 to 500 um in mean size compared with 1 to 3 mm for bubbling fluidized bed combustion operations). In view of the finer particles and higher superficial gas velocities, there is considerably more carryover of particles from the reaction chamber of circulating beds, and it is therefore essential to provide for continuous and efficient return of solids to the base of the reactor. The return system, usually consisting of a primary cyclone without a conical base and a sealed return line such as a fluoseal or L-valve, is an integral part of the reactor. Because of the high velocities, erosion of tube surfaces would be a severe problem for any horizontal surfaces inside the reactor chamber. Hence, internal surfaces are avoided and heat is extracted via membrane waterwall surfaces forming the containing surface.

Circulating fluidized beds share a number of advantages with bubbling beds, including:

(a) Sorbent materials like limestone or dolomite can be used as bed materials to capture sulphur in situ, reducing the emissions of SO2 and SO3.

(b) Because of the low temperatures of combustion (typically 750-950 C), emissions of NOx are also reduced considerably.

(c) Heat transfer coefficients are high between the bed or suspension and cooling surfaces, leading to compact equipment.

(d) The combustors are able to handle a wide variety of fuels (particulate, liquid or gaseous) in a flexible and interchangeable manner.

In addition, CFBC units have been claimed to have a number of advantages over bubbling beds, in particular:

(a) Combustion efficiencies are said to be higher, typically 98-99% compared with 90-96%.

(b) Because of the finer sorbent particles, sulphur capture is generally better.

(c) The use of staged air introduction in CFBC boilers leads to further reductions in NOx emissions.

(d) Improved lateral mixing of solids is said to lead to a requirement for fewer feed points, a major source of expense and engineering difficulties for underbed-fed bubbling bed boilers.

(e) Turndown and load following are claimed to be superior in CFBC units. Turndown can be achieved either by means of varying the suspension density for membrane surfaces on the wall of the reactor or by varying the proportion of solids circulated to an external cooler.

(f) The higher superficial velocities in CFBC units lead to a requirement for smaller combustor cross-sectional areas, although this is offset, at least for low capacity boilers, by the need for greater height.

Disadvantages of circulating beds appear to be that they require more solids preparation due to the finer materials required and that capital costs tend to be somewhat higher. Particulate emissions may also be harder to control because of the finer particles and higher gas velocities employed.

The original impetus for CFBC units and much of the development work have come from Europe, especially West Germany, Sweden and Finland. However, CFBC units are now being marketted vigourously in North America. With its extensive resources of coal, its widespread forestry operations, and the need to find means of disposing of a variety of waste materials (ranging from petroleum coke to municipal and hazardous wastes), Canada has a need to investigate CFBC technology. The Government of Canada has recognized this need, for example in subsidizing the cost of a prototype 22 MWe CFBC boiler for power generation at Chatham, New Brunswick.

In August, 1985 the authors of this report made an Unsolicited Proposal to the Government of Canada to investigate the burning of several low-grade fuels in a pilot scale circulating fluidized bed facility which was being constructed at the University of British Columbia. This proposal led to a 15 month contract whose scope was subsequently enlarged leading to an extension to 16 months, April 1, 1986 to July 31, 1987. This report details the results of the work carried out under the contract.

The original equipment, funded by a Strategic Grant from the Natural Sciences and Engineering Research Council of Canada, consisted only of a high temperature

circulating fluidized bed. The first part of the contract was therefore devoted to the addition of components (for solids feeding and for gas analysis) required to make the facility suitable for combustion trials.

Once the equipment had been completed and tested, the objectives of the work were to perform trial burns on a number of fuels which are of direct interest In Canada:

A Western Canadian coal.

One woodwaste material such as sawdust or hogfuel.

Two pitch or tar waste materials from heavy oil or tar sands upgrading processes. These materials are of considerable interest because they are produced as high molecular weight hydrocarbon wastes from hydrotreating and hydrocracking of unconventional feedstocks. The viability of these processes is affected by whether or not suitable processes can be found to dispose of the wastes, preferably with effective utilization of their calorific value through combustion to raise steam or generate electricity. Since the materials are difficult to handle and they contain corrosive materials like vanadium and nickel, they represent a challenge to the designer. Circulating beds are a possible technology for effective disposal and energy recovery from these materials.

Except in the case of the woodwastes, suitable limestones were to be used as sorbents in these trials.

In the course of the project, we were asked to include some trials on Minto coal from New Brunswick in order to produce waste solids which might be representative of those which would be generated at the Chatham facility. The limestone to be used in these trials was to be the Elmtree limestone from New Brunswick, one of the limestones to be tested with Minto coal in the Chatham CFBC unit.

The range of operations for the U.B.C. pilot plant Facility was specified as follows:

Superficial gas velocity	5 to 10 m/s
Excess air	10 to 20%
Bed temperature	800 to 900 C
Secondary to primary air ratio	1:2 to 4:1
Suspension density	10 to 50 kg/m3
Ca:S molar ratio	0 to 2

These values were chosen to be consistent with most current industrial practice.

Data and observations to be reported from the combustion trials on the various fuels were specified to be as follows:

(a) experience regarding fuel feeding, often a critical problem area;

(b) general operating experience and problems encountered in reaching and maintaining steady state combustion;

(c) temperature profiles through the system;

(d) combustion efficiency;

(e) NOx and SO2 concentrations in the off-gases;

(f) suspension-to-tube heat transfer coefficients;

(g) for the pitch or tar trials, chemical composition of the waste solids generated during the combustion at different points in the system.

In addition, we agreed to compare the overall performance of the different fuels investigated and to comment on any erosion or corrosion encountered.

2. THE EXPERIMENTAL FACILITY

An overall schematic of the experimental equipment is presented in Figure 2.1. The baghouse and secondary cyclone return were not, however, in place for any of the combustion tests. The various components are described in detail in the following sub-sections:

2.1 The Reactor

The principal reaction chamber is composed of five refractory-lined sections, each flanged. The five sections are assembled to provide a reaction chamber of cross-section 152 mm x 152 mm (6 inches square) with an overall height of 7.32 m (24 feet). A view of the reactor appears in Figure 2.2. The refractory is erosion resistant and is held in place by pins welded to the outer steel walls. The reactor is equipped with pressure taps and thermocouples at 610 mm intervals along opposite faces of the column. In addition, there are twelve regularly spaced 41 mm diameter ports which can be used as viewing ports or for insertion of probes or feed nozzles.

The distributor plate and plenum chamber are suspended from the bottom of the reactor for easy removal. Primary air is introduced to the bottom of the reactor through three tuyeres in the distributor plate. Each tuyere consists of a 38 mm o.d. stainless steel pipe, capped and drilled with six holes of 9 mm diameter inclined downwards at an angle of 30 degrees to the horizontal to prevent solids from flowing back into the plenum chamber during shutdowm. The distributor plate geometry is shown in Figure 2.3. An inclined stainless steel frame around the outer periphery of the grid plate protects the refractory at the base of the column from erosion.

Secondary air is fed to the reactor through four ports located 0.9 m above the primary air distributor plate. This secondary air can either be injected through two pairs of directly opposed orifices (ports a,b,d and e in Figure 2.4) or through four off-centre ports (b,c,e and f in Figure 2.4), the latter providing swirl. In the work reported in this report, the former configuration (directly opposed jets) was used exclusively. The primary and secondary air flows are controlled and metred separately so that their ratio can be varied with a fixed total air flow.

2.2 Air Supply and Preheating System

Air is supplied to the system by two building compressors located in the Mechanical Service area of the Pulp and Paper Centre. During the course of this work,

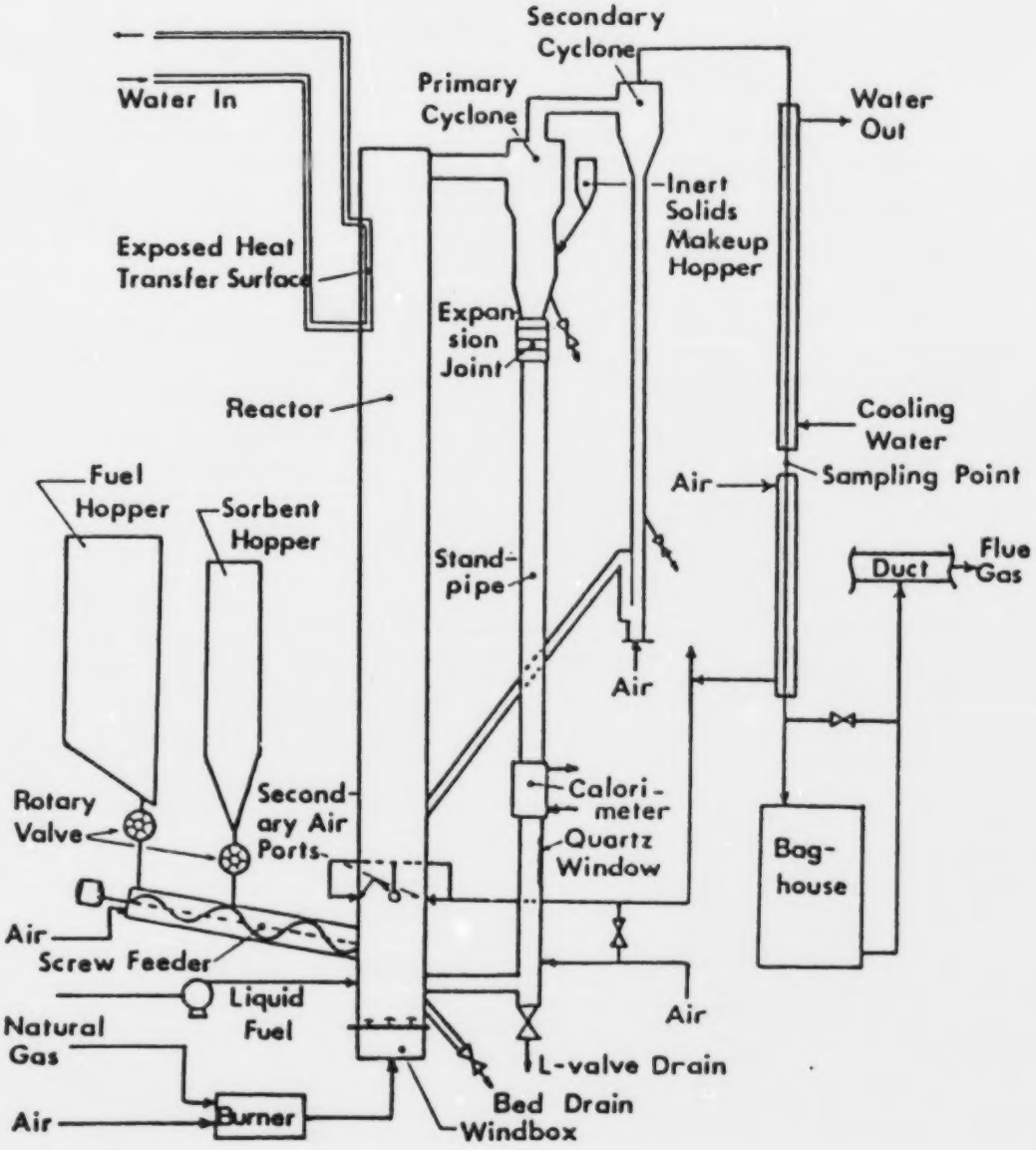

Figure 2.1: Simplified schematic diagram of experimental circulating fluidized bed combustion facility.

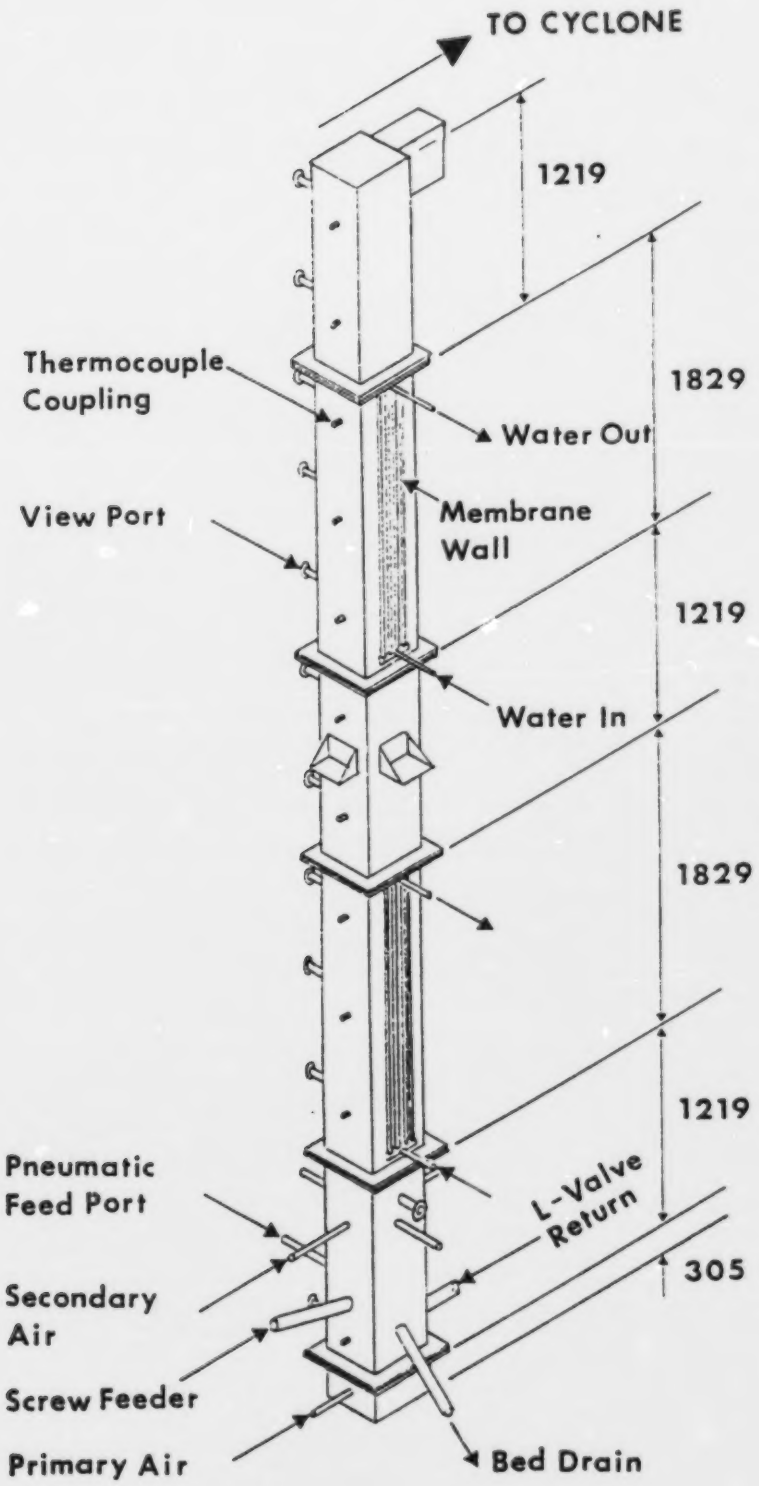

Figure 2.2: View of principal refractory-lined reaction chamber.

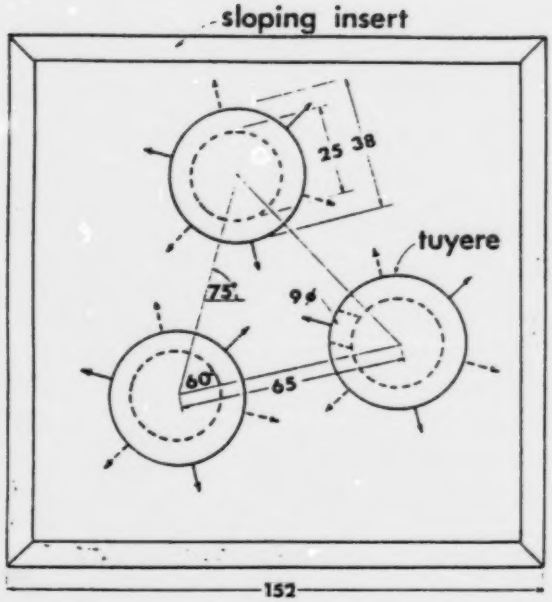

Figure 2.3: Distributor plate configuration. Solid and broken arrows refer to lower and upper holes respectively. All dimensions are in mm.

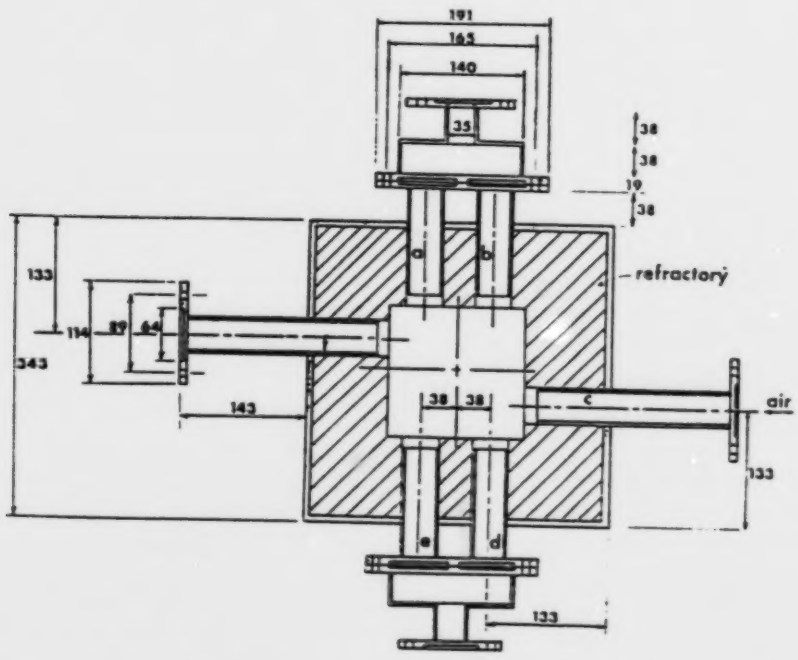

Figure 2.4: Secondary air inlet geometry. All dimensions are in mm.

several problems were encountered with these compressors as detailed in Chapter 3. Each of the compressors should have been capable of supplying 0.057 standard m3/s (120 scfm) at a pressure of approximately 600 kPa.

During start-up of the CFBC facility, it was necessary to preheat the primary air. This was accomplished in a cylindrical refractory-lined gas burner chamber of inside diameter 292 mm. Both natural gas and propane were available as preheating fuels, the former being preferred despite its maximum pressure of about 35 kPa gauge. The preheat burner was also employed during curing of the refractory, for some separate heat transfer studies and when solid or liquid fuel feeding was interupted to minimize heat loss.

2.3 Solids Feed System

As shown in Figure 2.1, the principal solids feed system consists of two large hoppers, two rotary valves and a screw feeder. The largest hopper was designed in such a way that it can, with minor modifications, be used either for feeding coal or other rounded particulates or for feeding difficult woodwastes like hog fuel. To accomplish this, the lowest section of the hopper and its rotary feeder are removed and replaced by a more gradually tapered bottom which empties directly into a slot at the top of the screw feeder to form a "live bottom". The two configurations are illustrated in Figure 2.5. Air is purged through the screw feeder and the hoppers are slightly pressurized to prevent backflow from the combustion chamber. In some of the early tests, pneumatic feeding was employed. This configuration is also shown in Figure 2.5.

The smaller of the two hoppers is a cylindrical vessel of inside diameter 305 mm and height 2.2 m. It discharges through a rotary valve which is used to control the flowrate. Both this rotary valve and the other one used for coal feeding from the larger hopper are equipped with rubber impellers to provide a seal and with transparent front plates so that the operator can tell if there is any problem with feeding. The screw feeder is intentionally oversized so that the solids feed rates (except for the wood wastes) are controlled by varying the rotational speed of the rotary valves. For most operating conditions with coal, it was found to be desirable to premix the coal and sorbent, with some in each of the hoppers. This provided a more accurate ratio of the two materials (and hence of the Ca:S ratio), and also provided a backup feed system in case a blockage should occur in either of the solids feed systems. Feed rates were determined by calibrating the rotary valves prior to the combustion runs with the bottom removed from the reactor so that fed solids could be caught and weighed.

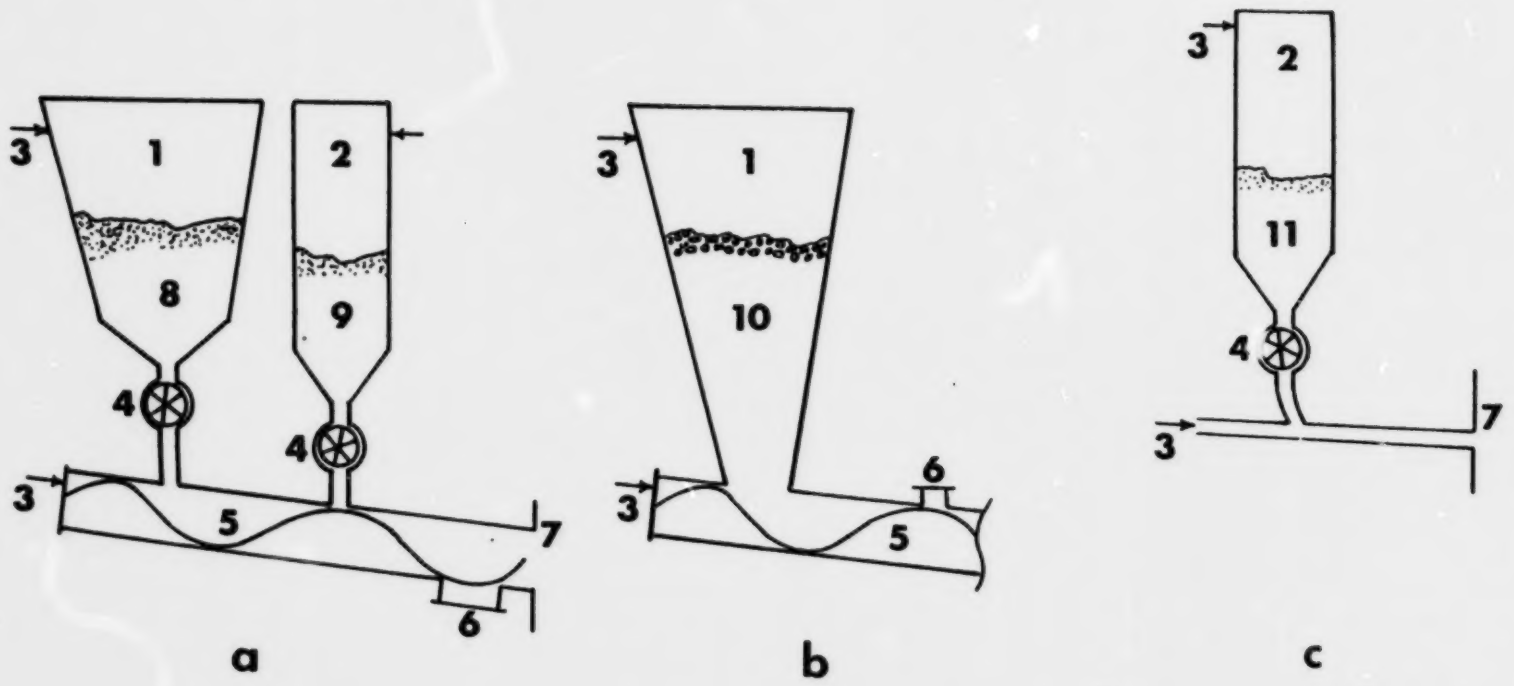

Figure 2.5: Solid feed configurations: a) Dual hopper for coal and sorbent with control by rotary valves; b) Live bottom hopper for woodwastes; c) Pneumatic feeding for coal/sorbent mixtures. 1: Large hopper; 2: Cylindrical hopper; 3: Air; 4: Rotary valve; 5: Screw feeder; 6: Blind flange; 7: Reactor; 8: Coal; 9: Sorbent; 10: Woodwaste; 11: Coal/sorbent mixture.

For runs with pitches (which were fed as liquids as discussed in the next subsection), limestone was charged to the smaller hopper. Because of the relatively small rate of solids feed in these cases, the outlet pipe from the rotary valve was then connected to a separately metred air line of diameter 10 mm, and the sorbent particles were conveyed pneumatically into the reactor at a height 710 mm above the gas distributor.

2.4 Liquid Feed System

Each of the three pitch materials investigated has a softening temperature between 100 and 170 C. It was therefore decided to feed these materials by first melting them and then pumping them into the reactor through a suitable nozzle. Considerable difficulty was encountered, especially with one of the materials, and a labourious and often frustrating trial and error process had to be surmounted before a workable system was devised. This system is shown schematically in Figure 2.6. The key elements of this system are as follows:

Preheating vessel: In order to prevent solid pitch from blocking the entrance to the feed pipe from the main heated reservoir, it was found to be essential to premelt pitch in a separate vessel, and then transfer the liquid by ladling to the main feed vessel. The premelting vessel had a capacity of approximately 0.12 m3 and was heated by a 1.5 kW electrical immersion heater and stirred by a 1/8 HP mixer impeller.

Main heated reservoir: This vessel had available three separate sources of heat which could be controlled independently to bring the contents of the vessel to temperatures as high as 200 C if required. Heat could be supplied by two 3.0 kW electrical barrel heaters on the outside of the vessel, by an immersed steam coil of surface area approximately 1.2 m2, and by a 3.0 kW electrical immersion heater near the outlet. The outside of the vessel was insulated using fibrefax wool. A ventilation hood with a small vacuum was installed over the top of the vessel. A small (1/2 HP) Lightnin mixer was installed at the top of the vessel to keep the contents in constant motion. The reservoir was supported on load cell type weigh scale with a digital readout to allow the flow rate of fuel to be estimated.

Piping system: The piping connecting the reservoir to the reactor was kept as short as possible. All sections were either heavily insulated or traced with high temperature electrical tape.

Nozzle: It was found to be essential to atomize the fuel as it entered the reactor. Several geometries were tested. The most successful was one which discharged obliquely upwards and had a fitting (see Figure 2.7) to allow rapid cleaning by means of a thin flexible rod.

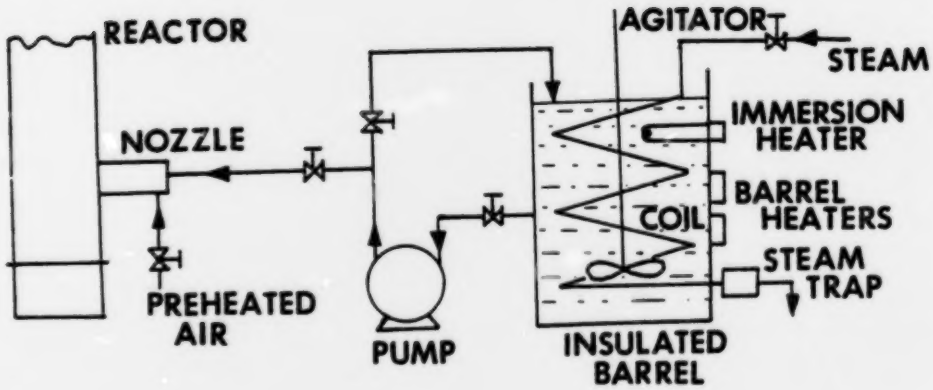

Figure 2.6: Liquid feed configuration.

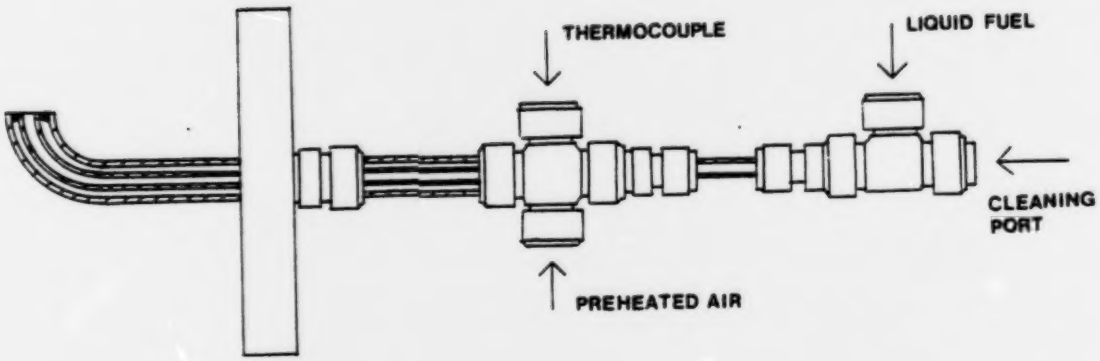

Figure 2.7: Nozzle for pitch feeding.

When discharging into air this gave a spray with an included angle of about 15 degrees. Atomization was achieved by using air which was heated in the calorimeter section of the L-valve (see section 2.6 below.) The configuration is shown in Figure 2.7.

2.5 Heat Transfer Surface

The reactor was constructed with two removable membrane waterwall heat transfer surfaces on one wall of the column, one beginning 1.22 m and other 4.27 m above the distributor plate as indicated in Figure 2.2. Each of the surfaces was comprised of four vertical stainless steel tubes of 21.3 mm o.d. and 13.9 mm i.d., separated by longitudinal flat fins welded along their lengths as shown in Figure 2.8. Thermocouples were positioned at 152 mm intervals inside one of the central tubes and at the inlet and outlet of the cooling water in order that heat transfer coefficients could be determined for different sections of the assemblies. Each of the cooling surfaces had a total exposed surface area of 0.30 m2 and a projected surface area of 0.23 m2.

In practice, for the fuels investigated in this study, it was found that too much heat was removed with both surfaces in place for the reactor to be brought up to a high enough combustion temperature (at least 800 C). The lower surface was therefore removed and replaced by a blank refractory section. Even with this single surface in place, it proved to be necessary to operate at very high superficial air velocities in order to sustain the temperature in the 850-900 C range. As a result, the upper surface was also removed for most of the combustion runs described in this report. It was replaced by a single stainless steel 19 mm o.d. vertical tube at the position of the upper removed membrane surface. This tube was normally positioned touching the refractory surface, but for some heat transfer tests it was also moved laterally in order to explore the influence of horizontal position on heat transfer coefficients.

2.6 Solids Recycle System

Gas and entrained solids leaving the top of the reactor enter a refractory-lined medium efficiency primary cyclone of inside diameter 305 mm. Solids separated in the cyclone drop into a conical recycle hopper which serves also as an inventory overflow vessel. Make-up inert solids can also be added into this vessel from a small adjacent hopper. From the bottom of this vessel, solids descend in moving packed bed flow in a 102 mm i.d., 4.42 m long externally

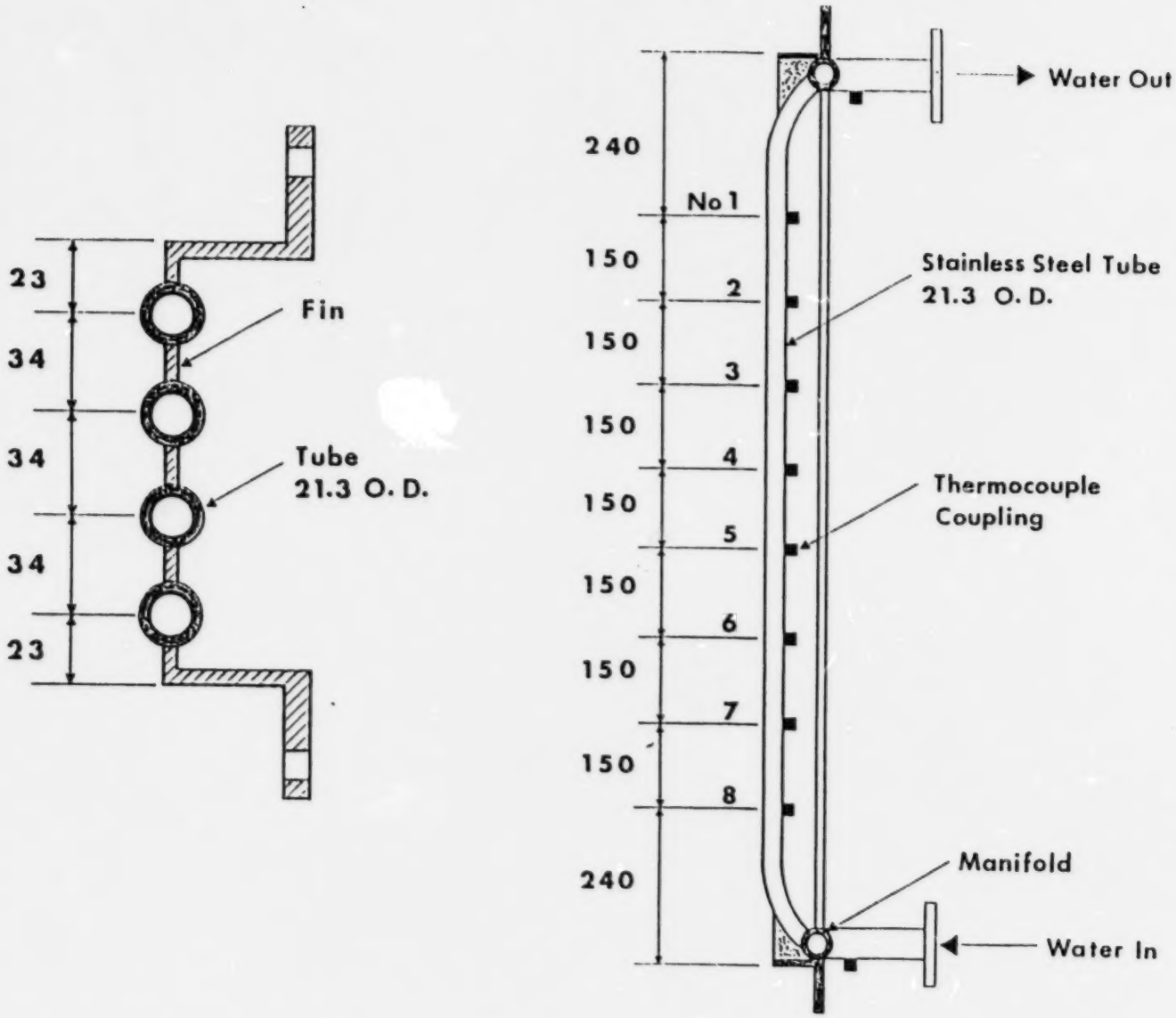

Figure 2.8: Membrane wall cooling surfaces: (a) plan view; (b) section view showing thermocouple positions. All dimensions are in mm.

insulated stainless steel standpipe, forming the vertical leg of an L-valve. Allowance for differential thermal expansion was made by having a bellows-type expansion joint near the top of the standpipe. The solids are returned to the principal reactor chamber 381 mm above the distributor plate through the horizontal leg of the L-valve. This leg is 810 mm long and 102 mm inside diameter.

The circulation rate of solids through the L-valve was controlled by the flow of aeration air which is added a single point just above the vertex of the L as recommended by Knowlton and Hirsan (1978). The circulation rate was measured by timing the passage of identifiable particles as they descended past a quartz window in the vertical standpipe section of the L-valve (see Figure 2.9). This window was also very useful for ensuring the state of flow of solids and provided an early indication if the inventory of solids was too low. The quartz window had a height of 331 mm and was flush with the adjacent stainless steel pipe; it began 730 mm above the bottom of the L. Solids circulation rates were calculated by assuming that the solids are moving in plug flow at their loose packed bed voidage along the standpipe. It has been shown by Burkell (1986) that this procedure gives accurate results providing that the measurement length begins at least two pipe diameters above the corner of the L.

Circulation rates could also be estimated by means of a calorimetric jacketted section of length 435 mm beginning 1.25 m above the bottom of the L-valve as shown on Figure 2.9. Either water or air could be used as coolant. In practice, air was generally used in order to minimize heat losses. As noted in section 2.3, this air, after heating in the jacketted section, was also used for atomization of liquid fuels. In this method a heat balance, in which the heat gained by the coolant is equated to the heat lost by the solids as they descend through the calorimetric section, is used to calculate the solids mass flow, i.e.

Solids mass flow = Coolant mass flow x Coolant specific heat x Coolant temperature rise / (Solids specific heat x Solids temperature rise)

Clearly heat losses and heat gained by the aeration air are ignored in this equation. Placement of the thermocouples used to measure the solids temperature at the entrance and exit of the section is critical to the accuracy of this method. This is discussed in detail by Burkell et al (1988).

Because measurements of solids circulation obtained by the quartz window method were more accurate than values obtained from the calorimetric section method, the

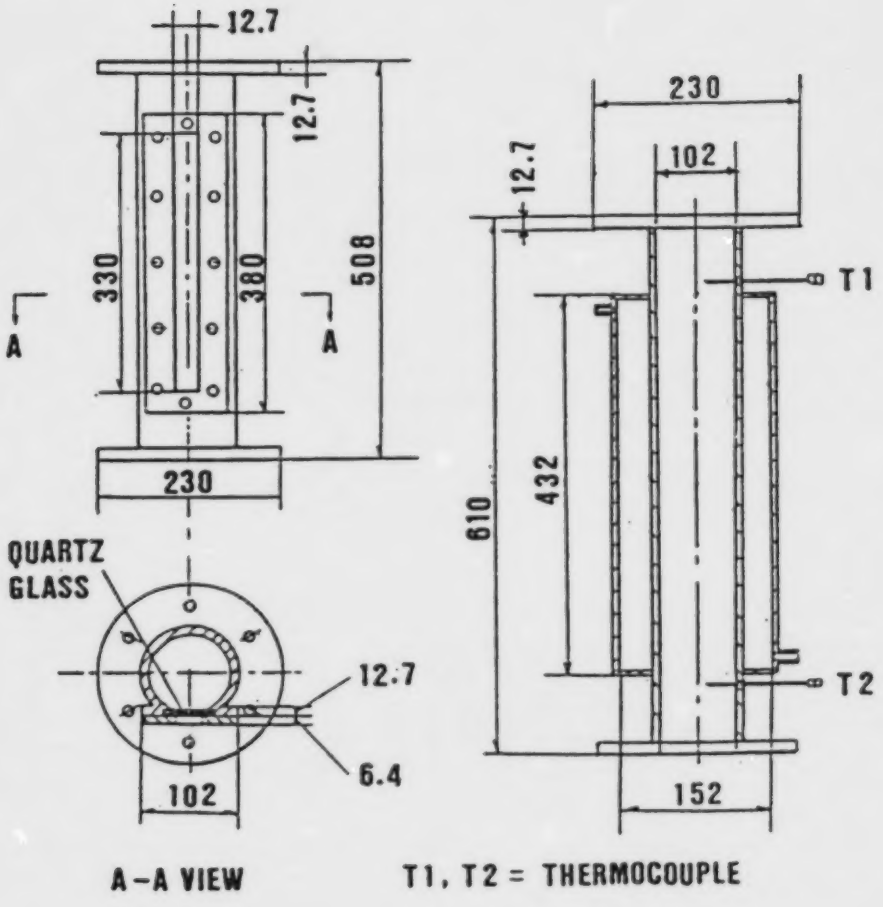

Figure 2.9: Quartz window and calorimetric section for measuring solids circulation rate. All dimensions are in mm.

former method has been used to determine all the solids circulation rates given in this report.

2.7 Gas Exit and Analysis

Gas and entrained solids leaving the primary cyclone were directed to a 203 mm i.d. high efficiency secondary cyclone, made of stainless steel and insulated externally. Solids captured in the secondary cylone were collected in a receiving vessel. Gas leaving the secondary cyclone was sampled for gas analysis, cooled in a U-tube heat exchanger and then discharged to the building ventilation system which is at a slightly negative pressure and has filters in advance of an induced draught fan.

The gas sampling system is shown schematically in Figure 2.10. Gas samples are directed to on-line analysers for measuring the concentrations of oxygen, sulphur dioxide, NO and NO2. Samples can also be collected with a syringe for injection into a gas chromatograph for analysis of carbon dioxide, carbon monoxide, unburnt hydrocarbons and confirmatory readings of sulphur dioxide concentrations. A modified Bosch lambda sensor type zirconia oxygen sensor was also tested (Hakansson, 1987) in the upper part of the reactor. In addition, another Bosch lambda oxygen probe was located in the duct between the primary and secondary cyclones for many of the tests. This gave an earlier indication of changes in oxygen concentration than the on-line sensor.

2.8 Solids Sampling

Solids were routinely sampled from three positions:

(a) through a ball valve at the base of the combustion chamber; these samples are referred to as "bed drain material" in this report.

(b) through a ball valve at the bottom of the standpipe which forms the vertical leg of the L-valve; these solids are termed "L-valve samples".

(c) by accumulation in the receiver below the secondary cyclone; these samples are designated "secondary cyclone samples".

In addition, small amounts of fine solids were recovered from the short horizontal leg of the U-tube heat exchanger which cools the exit gases (see Figure 2.1) after the run had beed concluded. These solids are referred to as "U-tube solids".

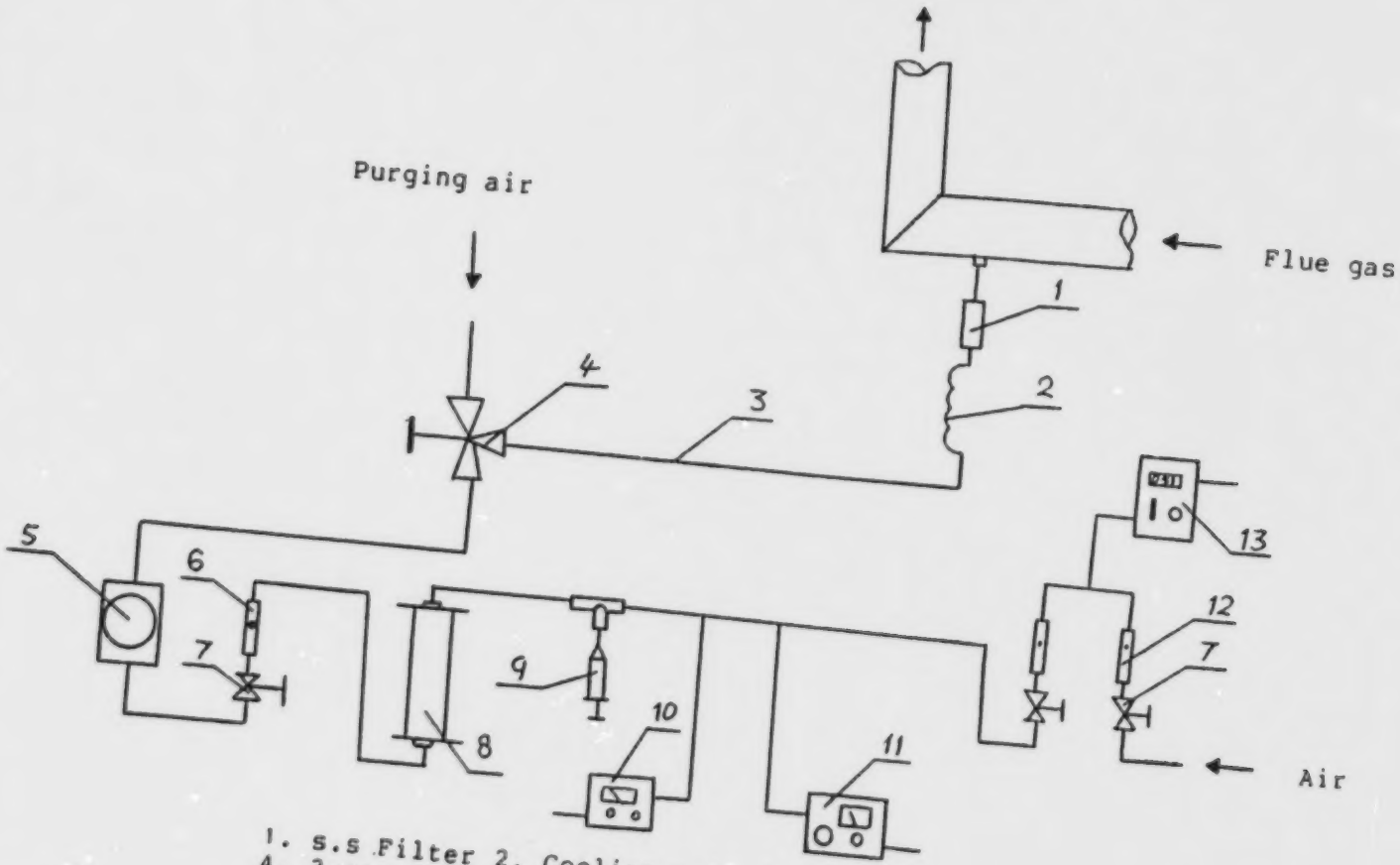

1. s.s Filter 2. Cooling coil 3. s.s. Sampling line
4. 3-way valve 5. Vacuum pump 6. Rotameter
7. Control valve 8. Drying tube 9. Syringe
10. Oxygen analyzer 11. NOx analyzer
12. Precision rotameter 13. SO_2 analyzer

Figure 2.10: Gas sampling system.

2.9 Instrumentation and Data Acquisition

In addition to the gas analysis system discussed in the previous subsection, instrumentation included:

(a) flow meters for measuring all air and water flow rates;

(b) thermocouples throughout the system (see Figure 2.11) to allow measurement of temperature profiles;

(c) pressure manometers measuring pressure drops over different intervals of the principal reaction chamber and absolute pressures at various points (see Figure 2.12.)

Data acquisition was provided by an AT&T 6300 computer equipped with a Metrabyte interface permitting 4000 samples per second in BASIC language and up to eight multiplexer boards with 16 channels on each board. Electrical outputs from the thermocouples were stored by the computer.

2.10 Properties of Fuels, Sorbents and Inert Particles

Test burns were carried out with a number of different solid fuels (three coals and two wood waste materials) as well as with two different pitches derived from oil upgrading operations. Proximate and ultimate analyses of the solid fuels are give in Table 2.1, together with heating values. Key chemical and physical properties of the two pitch materials appear in Table 2.2. Physical properties of the sorbents and inert sands employed in the experimental work are provided in Table 2.3. The chemical analysis of the sorbents and inerts used in this study are given in Table 2.4. All of these materials as fed belong in Geldart group B both at room temperature, according to the criteria established by Geldart (1973), and at the operating temperature and pressure of the combustor, using the criteria proposed by Grace (1986b).The ash compositions of two of the coals and of one of the pitches are presented in Table 2.5. Particle size analyses for the various particulate fuels, limestones and inert particulate materials fed to the unit before or during the combustion runs appear in Table 2.6. Most of the physical properties were determined at U.B.C., with particle size analyses being by sieving and, for the smallest particles, a Coulter counter. Proximate and ultimate analyses and ash analyses were carried out at the Centre for Mineral and Energy Technology (CANMET) in Ottawa, and generally show good agreement with previous reported values (e.g. Tibbets and Montgomery, 1976; Becker and Code, 1983; Couturier, 1986; Dearborn, 1986; Hamer et al, 1987) for the same materials.

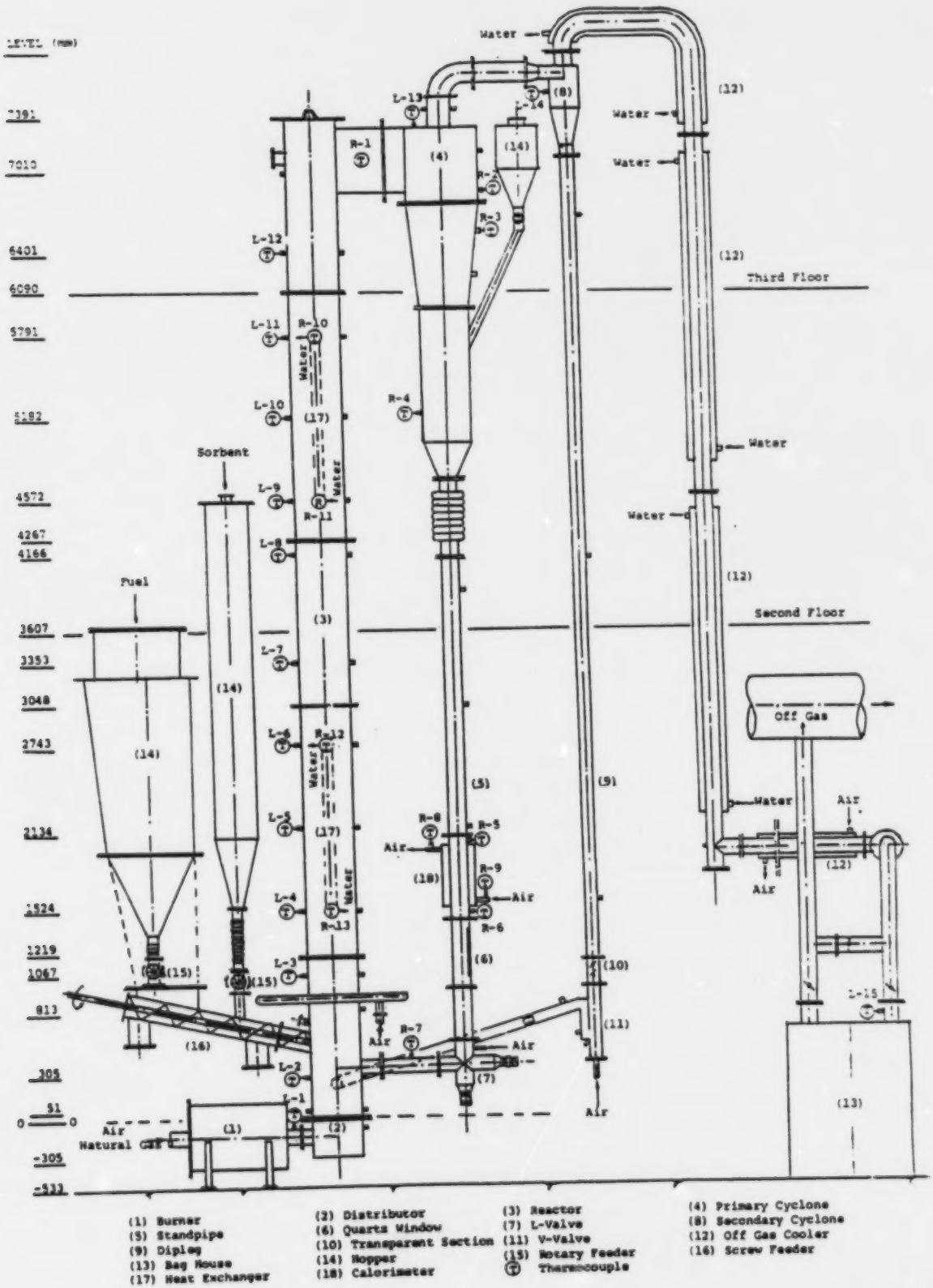

Figure 2.11: Thermocouple locations in CFBC reactor system.

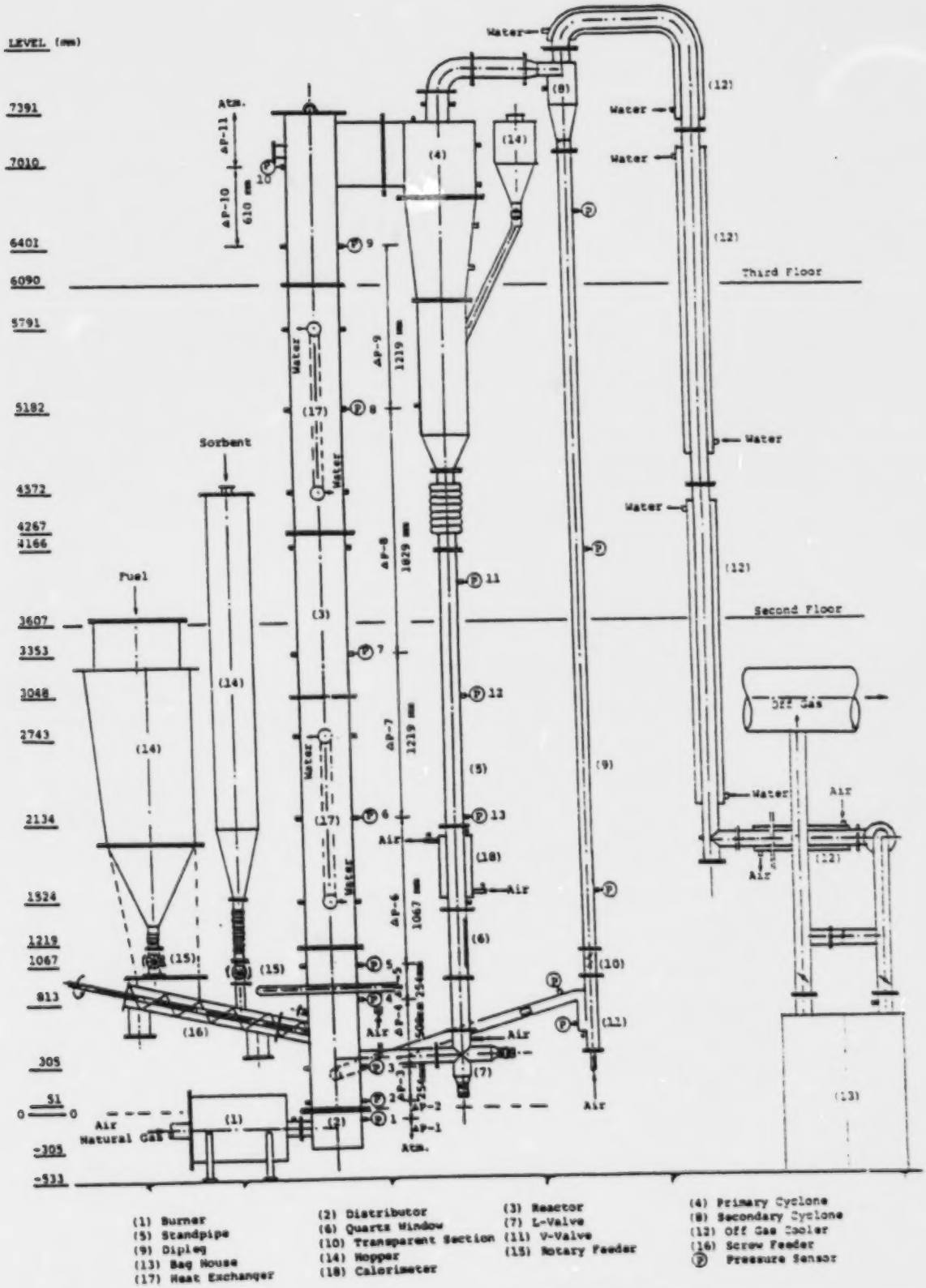

Figure 2.12: Pressure tap locations in CFBC reactor system.

Table 2.1: Proximate and Ultimate Analyses of Solid Fuels

	Esso Coal	Highvale Coal	Minto Coal	Hogfuel	Sawdust
Proximate Analysis:					
Volatile Matter	21.9	28.6	32.9	60.9	80.3
Fixed Carbon	64.3	35.0	46.8	23.9	12.6
Ash	13.1	16.6	18.8	4.0	0.4
Moisture	0.7	19.8	1.5	11.2	6.7
Ultimate Analysis (dry basis):					
Carbon	75.8	58.7	64.8	52.8	50.0
Hydrogen	4.2	3.9	4.2	5.4	5.8
Nitrogen	1.1	0.9	0.7	0.1	0.0
Sulphur	0.2	0.2	7.2	0.2	0.1
Oxygen (by diff.)	5.5	15.8	4.1	36.9	43.7
Ash	13.2	20.6	19.0	4.6	0.4
Higher Heating Value, MJ/kg	30.1	22.8	34.3	22.3	19.5

Table 2.2: Properties of Pitch Materials Tested

	CANMET Pitch	H-Oil Pitch
Proximate Analysis:		
Volatile Matter	67.7	
Fixed Carbon	30.2	
Ash	2.0	0.07
Moisture	0.1	0.01
Ultimate Analysis (dry basis):		
Carbon	86.2	86.4
Hydrogen	7.1	7.9
Nitrogen	1.1	1.0
Sulphur	2.8	2.3
Oxygen (by diff.)	1.0	2.3
Ash	1.8	0.1
HHV, MJ/kg	40.0	41.0
Physical Properties:		
Density at 15 C, kg/m3	1120	1131
API Gravity, 60/60 degF	<0	
PI, wt. %	55.1	
TI, wt. %	20.0	
Asphaltenes, wt. %	35.1	
CCR by MCR (RCR), %	56.4	43.2
GCD Data, % yield:		
IBP/204 C	0.0	
204/343 C	1.0	15.7
343/524 C	10.5	
524 C +	88.5	84.3

Table 2.3: Physical Properties of Particulate Materials

A) Inert Materials:

	Sand used in heat transfer tests	Sand used in heat transfer tests	Olivine 70 sand
Particle density in kg/m3	2637	2642	3066
Mean particle diameter, um	188	356	147
Voidage at minimum fluidization	0.46	0.42	0.46
Minimum fluidization velocity at room temperature in m/s	0.051	0.095	0.035

B) Sorbents:

	Elmtree lime	Texlime
Particle density in kg/m3	2400	2500
Mean particle diameter, um	210	214
Voidage at minimum fluidization	0.44	0.42
Minimum fluidization velocity at room temperature in m/s	0.041	0.044

Table 2.4: Chemical Analysis of Limestones and Inerts

	Elmtree limestone	Texlime	Olivine sand
CaO	54.32	54.57	0.41
SiO2	0.00	0.00	41.48
MgO	0.60	0.34	48.08
Fe2O3	0.56	0.45	8.58
Al2O3	1.43	0.62	0.76
SO3	N.A.	1.17	0.54
Na2O	0.05	0.05	0.05
K2O	N.A.	0.16	0.01
BaO	0.01	0.03	0.03
SrO	0.03	0.10	0.01
MnO2	0.08	0.01	0.00
TiO2	0.11	0.00	0.00
NiO	0.00	0.01	0.33
V2O5	0.00	0.00	0.00
P2O5	N.A.	0.00	0.00
Co3O4	0.00	0.00	0.00
MoO3	0.00	0.00	0.00
SnO2	0.00	0.00	0.00
ZnO	0.00	0.00	0.00
CuO	0.00	0.00	0.00

Table 2.5: Ash Composition of Fuels

	Minto coal	Esso coal	CANMET pitch	H-Oil pitch
SiO2	39.3	56.2	21.4	16.3
Al2O3	12.5	32.2	8.2	7.0
Fe2O3	39.8	1.7	44.9	24.0
CaO	2.6	2.6	6.8	3.5
MgO	0.4	0.8	5.4	3.7
Na2O	0.2	0.8	1.1	1.9
K2O	1.6	0.4	0.3	1.1
TiO2	0.6	1.9	0.7	0.7
P2O5	1.0	0.6	0.0	0.0
SO3	2.1	1.6	4.2	0.0
V2O5	0.0	0.0	3.6	25.5
NiO	0.0	0.0	1.1	12.0
CoO3	0.0	0.0	0.0	0.6
MoO3	0.0	0.0	0.0	3.9
ZnO	0.0	0.0	0.0	0.2

Table 2.6: Particle Size Distributions of Sorbents, Inerts and Solid Fuels

(a) Limestones and Inerts:

Interval, mm	Texlime wt. %	Elmtree limestone wt. %	Olivine 50 sand wt. %	Olivine 80 sand wt. %
-0.053+0.045	1.51	4.67	-	2.13
-0.090+0.053	2.91	7.99	0.20	5.44
-0.125+0.090	7.02	6.57	0.56	15.37
-0.180+0.125	19.76	6.74	0.98	33.09
-0.250+0.180	20.54	8.95	10.52	38.93
-0.355+0.250	13.19	10.86	26.97	4.53
-0.500+0.355	13.33	15.23	42.77	-
-0.710+0.500	14.06	16.69	17.66	-
-1.00+0.710	4.33	16.72	0.33	-
-1.40+1.00	0.95	4.69	-	-
-2.00+1.40	1.36	0.88	-	-
-2.80+2.00	0.61	-	-	-
-4.00+2.80	0.34	-	-	-
Mean diameter, um	214	210	356	147

(b) Solid Fuels:

Interval, mm	Minto coal wt. %	Sawdust wt. %	Hogfuel wt. %
-0.053+0.045	1.65	0.11	0.28
-0.090+0.053	3.99	0.80	0.93
-0.125+0.090	3.41	2.23	1.24
-0.180+0.125	3.74	3.56	1.52
-0.250+0.180	4.75	7.26	2.83
-0.355+0.250	5.48	11.38	4.20
-0.500+0.355	7.75	13.03	5.25
-0.710+0.500	8.73	16.31	5.71
-1.00+0.710	11.09	18.60	6.45
-1.40+1.00	12.11	14.43	6.25
-2.00+1.40	13.18	7.17	7.07
-2.80+2.00	10.92	3.04	7.77
-4.00+2.80	9.25	2.05	11.72
-5.60+4.00	3.50	-	10.18
-8.00+5.60	0.44	-	13.08
-11.0+8.00	-	-	4.20
-13.0+11.0	-	-	3.47
-14.0+13.0	-	-	1.03
+14.0			6.82
Mean diameter, um	388	442	847

3. EXPERIMENTAL PROCEDURES AND PROBLEMS ENCOUNTERED

3.1 Start-Up of the Unit

The circulating bed requires a longer time to achieve steady state temperatures than conventional bubbling bed combustors, because heat-up of the return portion of the cycle loop can only be achieved by the solids which are in free fall or moving packed bed flow. Heat transfer coefficients for transfer to the standpipe and lower leg of the L-valve are then much lower than within the principal reactor chamber.

Before start-up of the U.B.C. unit, approximately 100 kg of inert material, usually an olivine sand with a mean particle size of either 149 um or 356 um, is charged to the conical recycle hopper at the top of the return loop through the small feed hopper there (see Figure 2.1). Other preparatory action includes cleaning of the U-tube heat exchanger, and duct exit, changing the filters in the mechanical service area and in the sampling line, calibrating the feeder system for the particular fuel, and generally checking the entire system.

Start-up of the combustor is initiated by adjusting the air flow rate and natural gas or propane flow to provide a temperature in the preheat burner chamber of about 900 C with a superficial gas velocity in the reactor of about 5 m/s. The inert solids are then circulated through the system to bring the overall temperature up to about 400 C, a process which requires about four hours. Just enough secondary air and screw feeder air are fed during this stage to keep the orifices unblocked. Cooling water flows to the in-bed heat exchanger and to the U-tube aftercooler are initiated when the temperatures in those vicinities exceed about 200 C.

Once the temperature in the entire system exceeds 400 C, the primary air flow is decreased to a point where a dense bed is formed on the distributor. With the windbox temperature maintained at about 900 C, the dense bed is then heated to a point (525-750 C depending on the fuel) where ignition of the solid or liquid fuel can be sustained. Fuel feeding is then initiated, slowly at first. With ignition occurring in the lower part of the bed (confirmed visually through the lower viewports and by rapid rise in the temperature at the thermocouples in this region), the temperature is restrained by employing pulses of L-valve aeration air to inject slugs of cooler solids into the reactor from the L-valve. A careful process is then followed where the solid or liquid feed rate is gradually increased, the natural gas or propane rate is gradually decreased to 0 and L-valve aeration is increased, until the entire system operates with minimal intervention from the operators. Caution must be exercised when the natural gas

burner is being used that the absolute pressure in the burner does not exceed the line pressure of the natural gas, about 35 kPa, or violent surges occur. Observations through the quartz window in the vertical standpipe of the L-valve (see section 2.6) are very helpful in judging the state and steadiness of the solids recycle flow. When sorbent is required for sulphur capture and the sorbent is not premixed with the fuel, sorbent feeding is initiated once the average temperature of the system has reached 750 C. The secondary-to-primary air ratio is gradually increased during the heat-up phase, being established in the agreed range (1:2 to 4:1) before steady state operation is achieved.

The overall heat-up period, from turning on the gas burner to achieving temperatures throughout the reactor and return leg system above 850 C, required a total time of 10-13 hours when no serious problems were encountered. Once the correct temperature was reached, the flow rates were adjusted to match predetermined values, but with small changes where needed to bring the concentration of oxygen in the flue gas into the range 3.0 to 4.5 % by volume. At the same time, the solids circulation rate were corrected by means of the L-valve aeration setting to keep the temperature as close as possible to the desired levels. Once the desired temperature was reached, the secondary cyclone solids receiver was emptied. Solids were also drained periodically from the L-valve and bed drain ball valves (see section 2.8). For runs with high sulphur fuels, enough time had to pass for the equivalent of three times the initial inert mass of the solids to be discharged before solids samples could be retained. For the Minto coal runs, for example, it required a period of 8-12 hours, depending on the Ca:S ratio, to reach what was considered to be steady state in the composition of the solids. The receiver for solids from the secondary cyclone was then emptied again.

3.2 Solids Sampling Procedures

Bed drain and L-valve solids samples were discharged into stainless steel containers. The initial discharge was discarded to avoid material that had been sitting in or just above the valve. As soon as the sample to be retained had been collected, fibrefax insulation was inserted to completely cover the sample and prevent contact with air while the sample cooled. When cooled to room temperature, the samples were transferred to plastic or glass containers and sealed for transportion, analysis or storage. Secondary cyclone samples were obtained by diverting the flow which normally goes to the receiving vessel through a Y by means of two gate valves to a smaller container which was held in place for long enough to collect the requisite amount of material.

3.3 Problems Encountered

During the course of the experiments a number of problems were encountered which required special corrective action. The key ones were as follows:

(a) Compressor Problems: This project was the first major user of the building compressed air supply in the new U.B.C. Pulp and Paper Centre. The compressors proved to be very troublesome:

(i) Overheating occurred on warm summer days causing the compressors to trip out.

(ii) The capacity of the compressor system was lower than required by the building specifications.

(iii) Oil from the compressors frequently entered the air feed lines and rotameters in quantity.

Changes were made in the temperature settings and in the ventilation of the compressors. The building architects and mechanical contractors also agreed to change the compressors to a more suitable model.

(b) Heat Loss: As discussed in section 2.5, heat losses from the column proved to be excessive with membrane surfaces present in the combustion chamber. This was solved by removing both membrane cooling surfaces and replacing them by a single cooling tube. In addition, extra external insulation was added to the L-valve, especially to flanges.

(c) Thermal Expansion: In early operation of the unit, it proved to be difficult to maintain alignment of the rotary solids feeders (see section 2.3) due to thermal expansion of the reaction chamber. This was corrected by replacing the direct coupling drives by chain drives. The support system of the principal reactor was also improved, making it easier to maintain vertical alignment at all times.

(d) Blockage of Secondary Cyclone Receiver Connecting Pipe: With some materials that tended to be sticky, for example the fines from the Minto Coal trials and those from H-Oil pitch, the 50 mm pipe connecting the bottom of the secondary cyclone to the receiver vessel tended to bridge and become blocked. Deblockage could be achieved with the aid of a plumber's auger and percussion. A larger connecting pipe will be installed for future tests.

(e) Sintering in the Reactor: Two of the fuels, Minto coal and CANMET Pitch, gave some sintering problems in early runs. Sinters had to be removed in several cases by allowing the reactor to cool and removing the distributor plate. Successful corrective action included replacement of the original sand by an olivine sand, greater care to assure that the temperature in the lower part of the reactor never exceeded values of about 950 C, stricter control of oxygen concentrations during the start-up phase, increasing the overall superficial gas velocity, especially the primary

component, and increasing the flow of purge air along the screw feeder to promote adequate dilution and dispersal in the region near the solids feed point. Starting up with coal to bring the temperature up to a high level before pitch feeding was also helpful with the pitch materials.

(f) Water Pressure: On two occasions, interruption in the water supply to the laboratory occurred during experiments, apparently due to excessive water usage in the city and a mains problem. Since we rely on water for cooling of the in-bed tube and of the flue gases, this caused problems, in the first case leading to damage on welds in the U-tube cooler. The Pulp and Paper Centre, being at the end of the water line, will have a booster pump installed. In addition, an alarm system will be added for future experiments.

(g) Hot Spot: On one occasion, a hot spot developed on the wall of the reactor chamber when a piece of refractory near the distributor chamber came away allowing hot gases to reach the steel shell. The run was immediately aborted, and the damage repaired after the system had completely cooled.

(h) Feed Problems: For the most part, the solids feed system performed well, except for the alignment problem on the rotary valves described under (c) above which plagued early tests. Some difficulty was, however, encountered with the woodwaste materials in maintaining a steady flow. Installation of a rotating impeller in the bottom of the large hopper and use of vibrations allowed us to surmount this problem. Problems with pitch feeding proved to be considerably more difficult to overcome, particularly with CANMET Pitch which tended to freeze and/or coke at every opportunity. The measures finally adopted to solve this problem are detailed in section 2.4.

(i) Blockage of Building Ventilation System: For pitch #3 we found that considerable fine solids penetrated beyond the secondary cyclone, leading to collapse of the filters in the Mechanical Service area and positive pressures in the ventilation system. A baghouse has been purchased and will be installed prior to future experimental runs. This should overcome this problem.

3.4 Shutdown of the Unit

The unit was shut down by cutting off the supply of fuel, while maintaining the air flow, until the temperature at every point in the reactor had fallen below 400 C. In the case of the woodwaste runs where there was no rotary valve to provide a seal between the hopper and the reactor, special care was taken to increase the purge air flow through the screw feeder during shutdown.

4. HEAT TRANSFER AND TEMPERATURE PROFILES

4.1 Heat Transfer Coefficients

As shown by Grace (1986a), there has been a dearth of information on circulating bed heat transfer coefficients. Initial experiments were carried out to gain experience with the overall equipment and to obtain results on heat transfer coefficients between the membrane surfaces and the fast fluidized bed suspensions under different operating conditions. Subsequent data were also obtained during combustion runs at full combustion temperatures, most of these data being for the single vertical tube immersed in the upper part of the reactor chamber. Since there was never any evidence that the heat transfer results differed in any appreciable manner from one fuel to the next, the heat transfer results are presented in a unified separate section rather than as sub-sections when discussing the combustion of individual fuels.

4.1.1 Membrane wall measurements

The first group of experiments was carried out at temperatures low enough that radiation plays a secondary role, with heating supplied by burning natural gas in the preheater chamber. Average suspension to membrane heat transfer coefficients are plotted against suspension densities in Figures 4.1 and 4.2 for sand particles of mean diameter 188 and 356 um, respectively. Particle size distributions for these materials appear in Table 4.1. The suspension densities plotted in Figures 4.1 and 4.2 are cross-sectional mean values estimated from measured pressure profiles, ignoring all terms except that due to gravity. This procedure is commonly used as a first approximation in circulating fluidized bed systems. The open and blacked-in symbols refer to the total upper and lower membrane surfaces, respectively. All heat transfer coefficients here are based on the total exposed heat transfer surface area.

In both Figures 4.1 and 4.2, the heat transfer coefficient increases with the suspension density. In Figure 4.1, there is seen to be little influence of changing the secondary-to-primary air flow ratio over the range of 0 to 1.5. In both figures, there appears to be no systematic difference between the upper and lower exchange surfaces. Comparing the two figures, we find that the results for the two sands are almost identical, except at low suspension densities where the smaller particles gave somewhat higher heat transfer coefficients.

Figure 4.3 shows the variation in the suspension-to-surface heat transfer coefficients as a function of superficial gas velocity for the 188 um sand particles. The

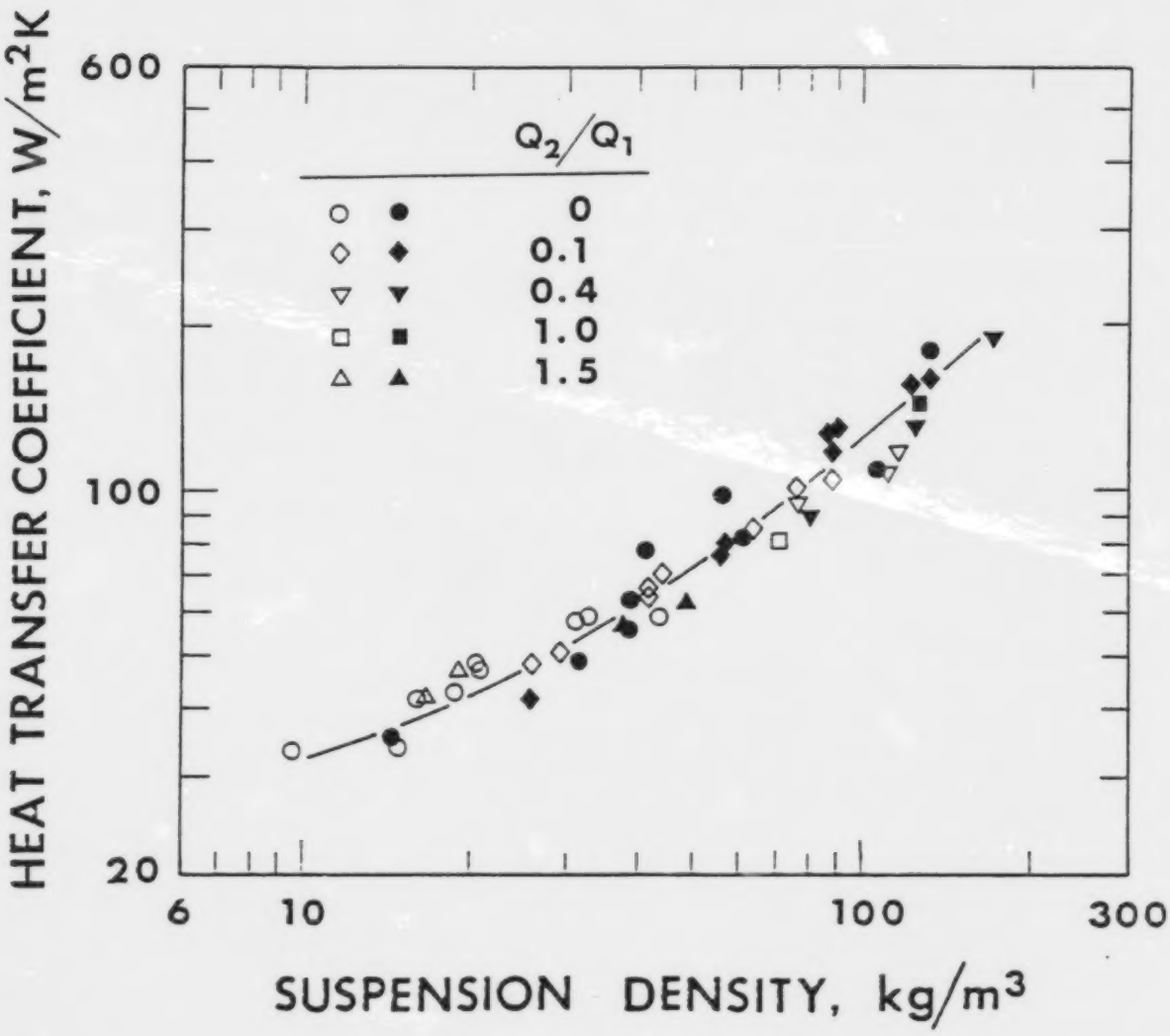

Figure 4.1: Average suspension to membrane wall heat transfer coefficient for 188 μm particles as a function of suspension density for different secondary/primary flow ratios. Open and closed symbols refer to the upper and lower exchange surfaces respectively.

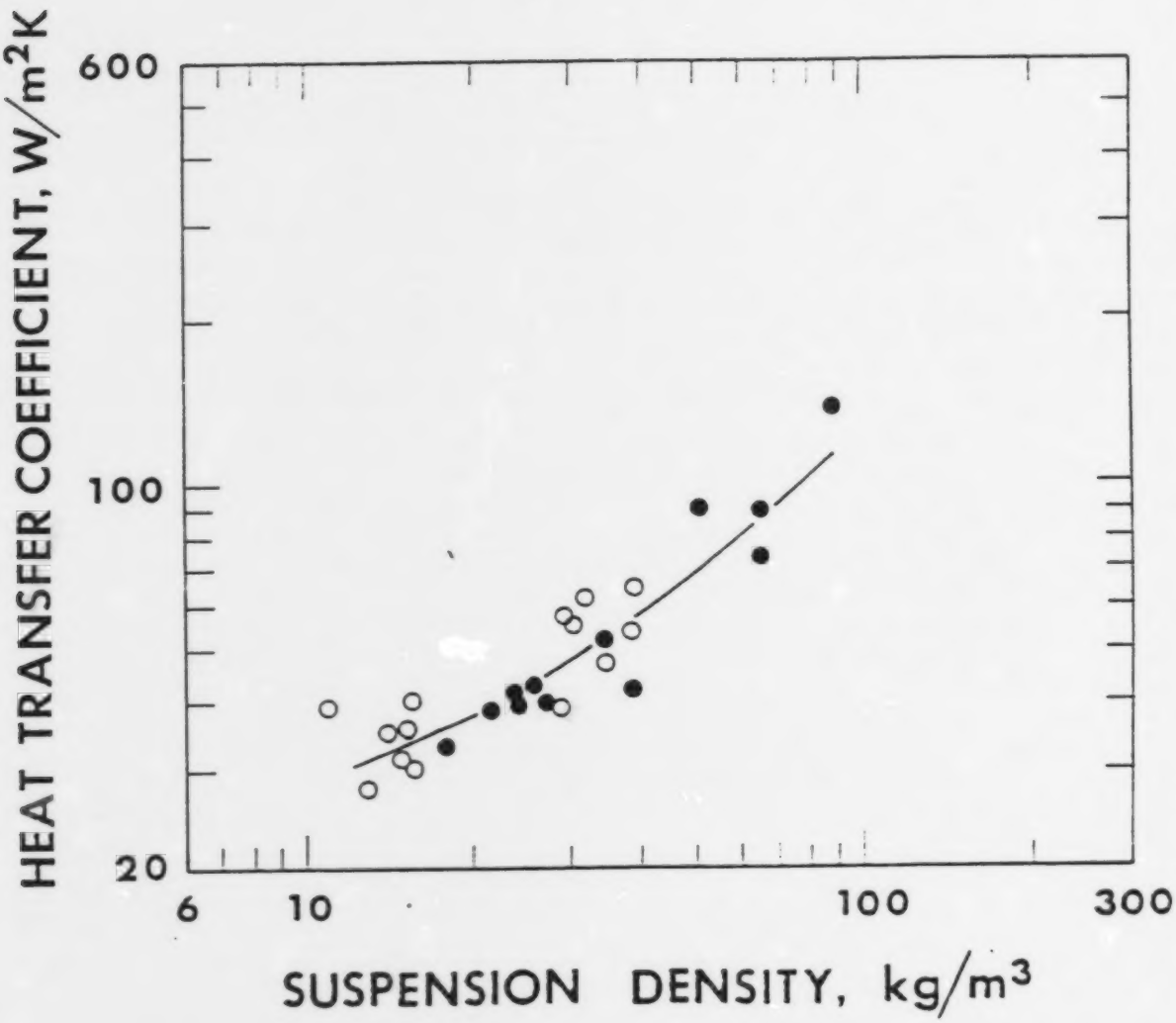

Figure 4.2: Average suspension to membrane wall heat transfer coefficient for 356 μm sand particles as a function of suspension density. Secondary/primary air ratio = 0 for all cases. Open and filled symbols refer to upper and lower heat transfer surfaces respectively.

Table 4.1: Particle Size Distributions of Sand Used during the Heat Transfer Experiments

Interval, mm	Fine Sand	Coarse Sand
-0.053+0.045	0.1	-
-0.061+0.053	0.3	0.1
-0.090+0.061	0.9	0.1
-0.106+0.090	3.3	0.2
-0.125+0.106	5.4	0.3
-0.150+0.125	11.4	1.0
-0.180+0.150	13.4	1.3
-0.208+0.180	20.4	3.0
-0.250+0.208	21.8	4.0
-0.297+0.250	10.1	5.8
-0.351+0.297	6.0	19.7
-0.420+0.351	2.2	20.7
-0.495+0.420	2.4	27.2
-0.600+0.495	1.8	14.2
-0.850+0.600	0.6	2.4
Mean diameter, um	188	356

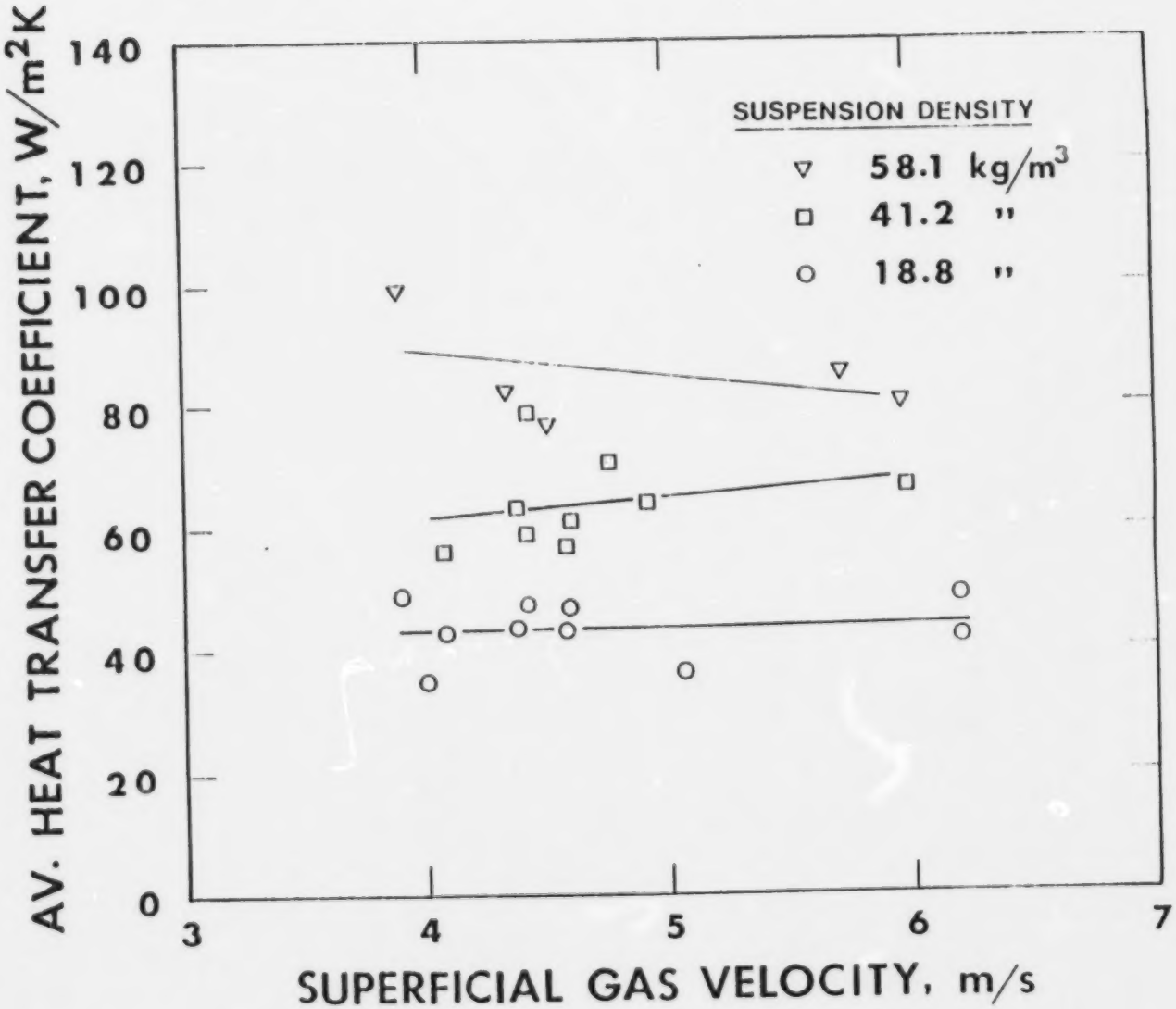

Figure 4.3: Influence of superficial gas velocity on average suspension to membrane wall heat transfer coefficient at three different suspension densities for the 188 um sand.

lines plotted are least-squares regression lines for each suspension density. It is seen that the superficial gas velocity does not significantly affect the heat transfer coefficient once the suspension density is established. This arises because the contribution of gas convection to the heat transfer is much less than the contribution of particle convection (Grace, 1986a).

Having thermocouples along the length of the membrane surfaces allowed heat transfer coefficients to be determined for part-lengths along the surfaces. Figure 4.4(a) shows that the local heat transfer coefficient for the upper membrane surface decreases quite rapidly with decreasing height, i.e. with increasing distance measured downwards from the top of the cooling surface. The trend is quite different in Figure 4.4(b) for the lower membrane surface. In this case, the coefficients reach a minimum in the central part of the surface. The difference is probably due to different solids flow patterns over the two surfaces. For the upper surface, the predominant solids flow, as observed in the cold model work described by Brereton (1987) for example, is downward in sheets in the wall region and upward in dilute flow in the core. In this case the downward moving sheets would progressively give up their excess heat as they move along the cooling surface, thereby decreasing the driving force for further transfer. The fact that the heat transfer coefficient is approximately proportional to the square root of the distance measured downwards from the top of the surface suggests that particle renewal in the downward-moving sheets is minimal. In the lower part of the column, the particle motion is much less regular with the particles moving both upward and downward. This accounts for the minimum in the heat transfer coefficients in the centre of the lower membrane surface. The increase in the suspension density over the lower part of the surface (see Figure 4.4(b)) probably also contributes to the sharp increase in the heat transfer coefficient near the bottom of the lower surface.

These findings indicate that the length of the heat transfer surface plays a significant role in determining the overall transfer coefficient. Small heat transfer probes will tend to give misleadingly high heat transfer coefficients since the particles at the surface will not have time to reach thermal equilibrium with the surface. Since almost all previous results are for very small surfaces, this could lead to an under-design of the required heat transfer surface area. Moreover, for long surfaces, the influence of particle diameter will be relatively small since the temperature gradient will have extended inwards over many particle diameters, whereas for small surfaces the particle diameter will be important since the heat transfer will only affect the initial layer of particles. These points are discussed at greater length by

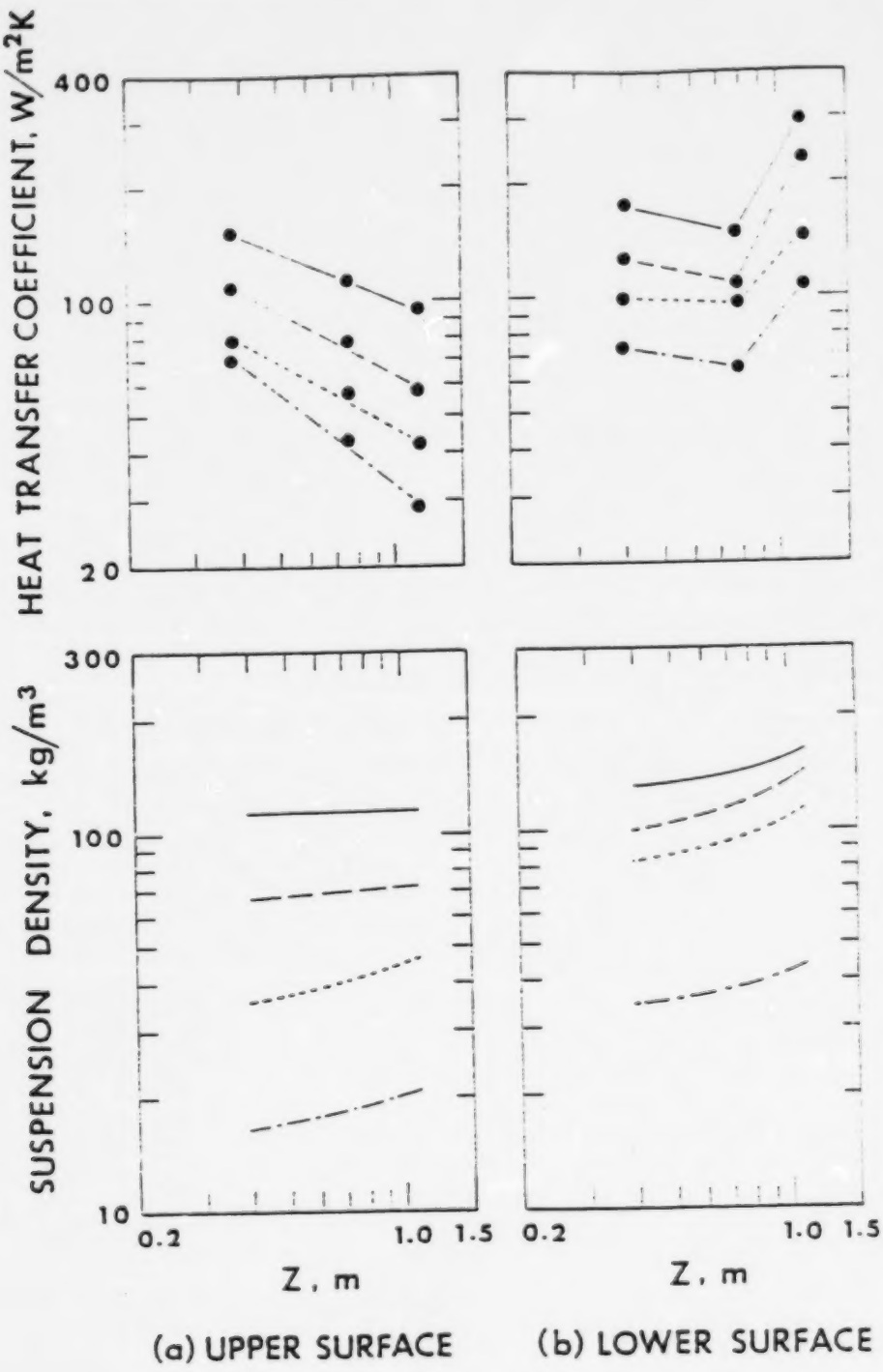

Figure 4.4: Typical longitudinal profiles of heat transfer coefficient and suspension density for (a) upper surface, and (b) lower surface. Coefficients are obtained between thermocouples 1-3, 3-6, 6-8 in Figure 2.8(b) for 188 um sand particles.

Glicksman (1988). Figure 4.5 shows that particle size indeed plays a significant role when a comparison is made between results for the two sands for measurements only over the top 305 mm for the upper membrane surface.

Additional heat transfer measurements at low temperatures are reported by Wu et al (1987).

As noted in section 2.5, most of the combustion studies were carried out with both of the membrane surfaces removed and replaced by a single tube. However, some measurements were obtained with the uppermost membrane surface under combustion conditions, i.e. temperatures of 750-850 C. Typical results are shown in Figure 4.6 in comparison with the results obtained at much lower temperatures where radiation is not a factor. It is seen that radiation contributes about 60 W/m2K for the conditions studied. The contribution of radiation is considered further below for the tube measurements.

4.1.2 Single vertical tube measurements

Most of the measurements with the single stainless steel vertical heat transfer tube were obtained with the tube touching the near wall of the column. For some of the measurements, the tube was pushed in so that it was located at other radial locations. In these cases, a correction was made for the horizontal sections of tube leading to the top and bottom of the vertical section of interest. All heat transfer measurements therefore apply to the entire vertical section of the tube. Suspension densities were estimated from pressure profiles as before.

Overall heat transfer coefficients are plotted in Figure 4.7 as a function of suspension density and suspension temperature at the height corresponding to the centre of the tube, located adjacent to the wall. While there are small differences in the superficial velocity of the gas for the different symbols, this effect is small as already shown. For all cases, the heat transfer coefficient is seen to increase with increasing suspension density and with temperature. Since radiation is essentially nil for the lowest suspension temperature investigated, the difference between this curve and the other curves gives a good estimate of the contribution of radiation. Note that the somewhat larger particle size for the lowest curve may also have contributed somewhat to the lower heat transfer coefficients for the suspension temperature of 368 C. Figure 4.8 shows a cross-plot of the same data as plotted in Figure 4.7 against temperature for three suspension density levels.

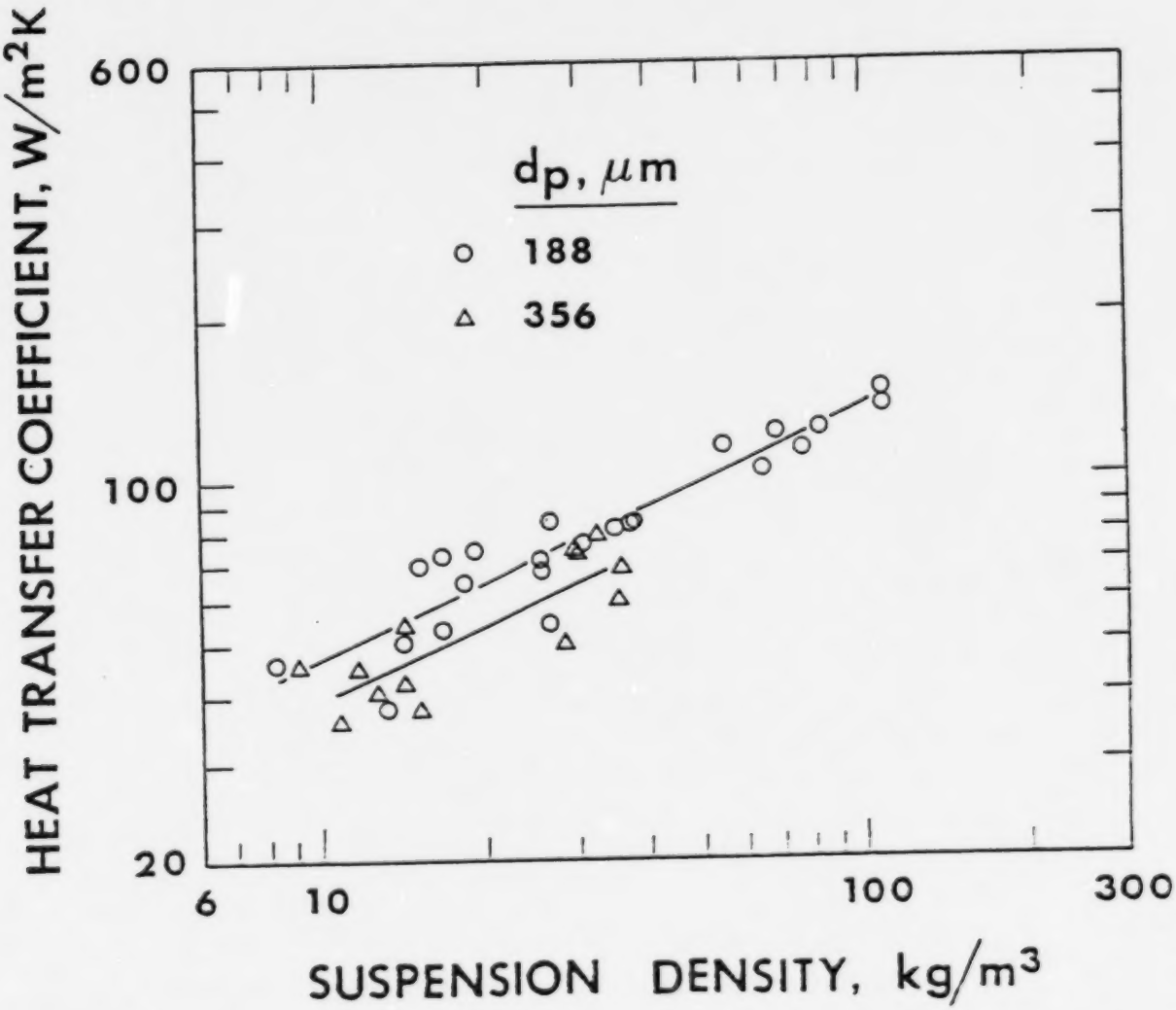

Figure 4.5: Heat transfer coefficient for section of upper heat exchange surface between thermocouples 1 and 3 in Figure 2.8(b) for two sizes of sand.

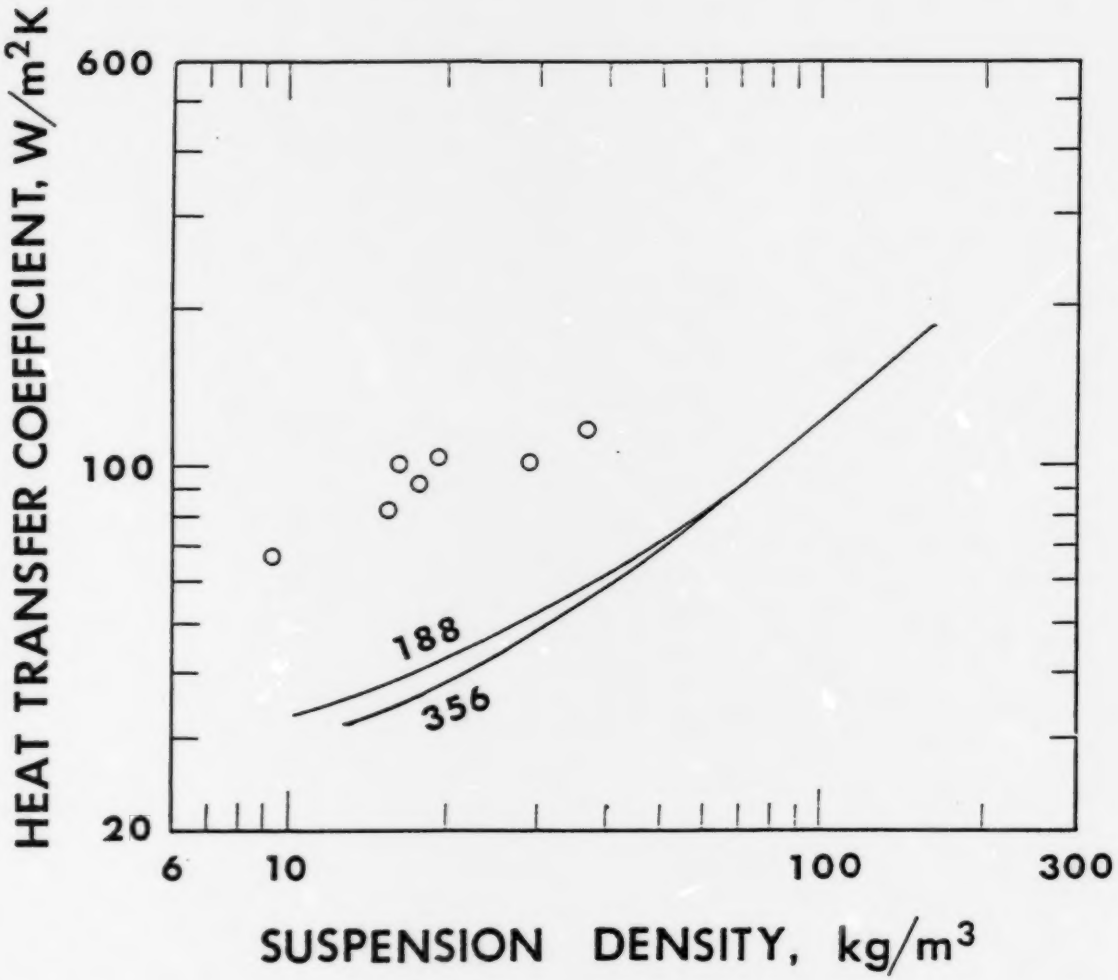

Figure 4.6: Suspension to membrane wall heat transfer coefficients at combustion temperatures (750-850 C) for 303 μm mean particle size and U = 6-10 m/s (shown by points), compared with lines obtained under low temperature conditions (150-400 C) where radiation is negligible.

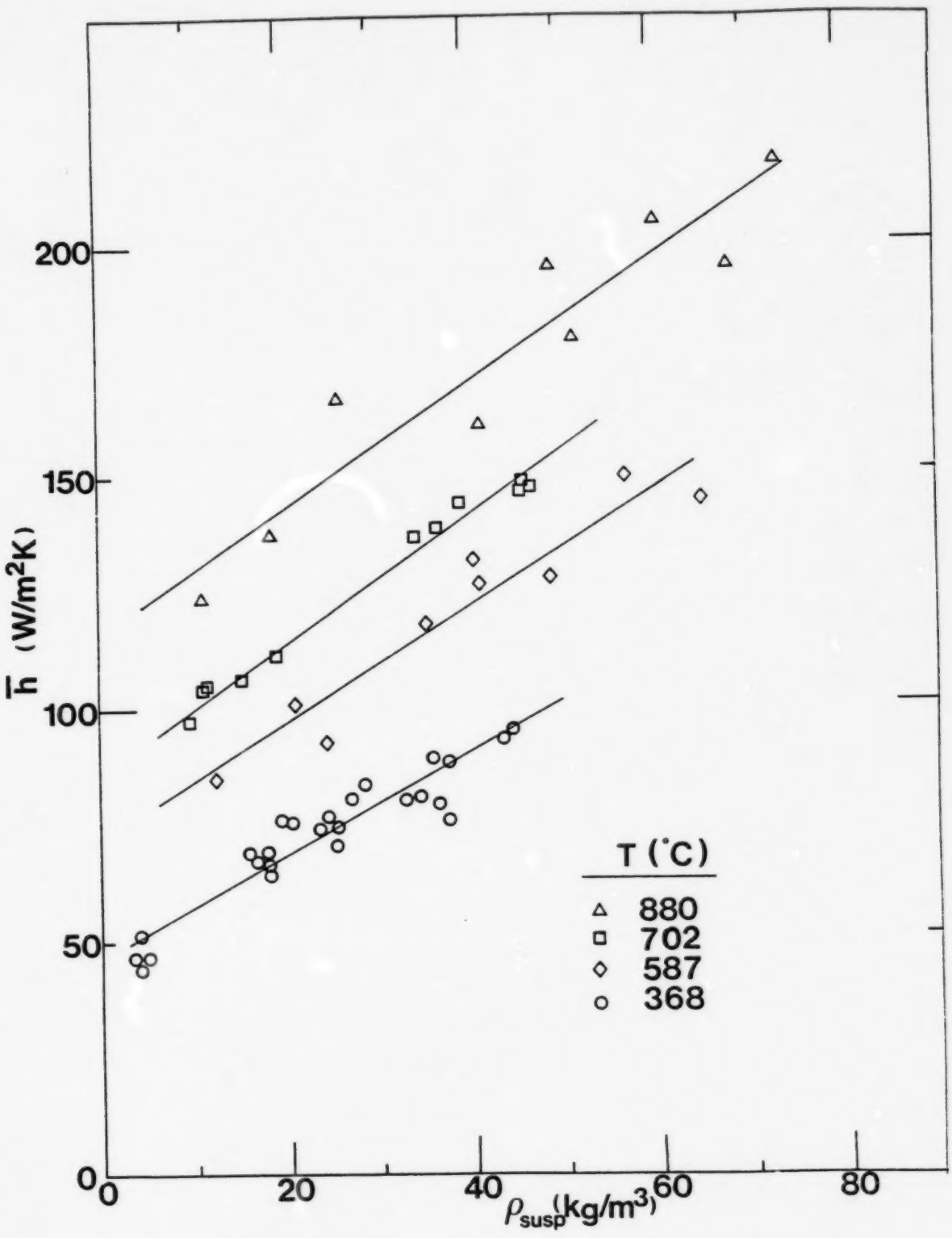

Figure 4.7: Suspension to vertical tube heat transfer coefficients for elevated temperatures, U = 6-8 m/s and mean particle diameter 250-300 μm.

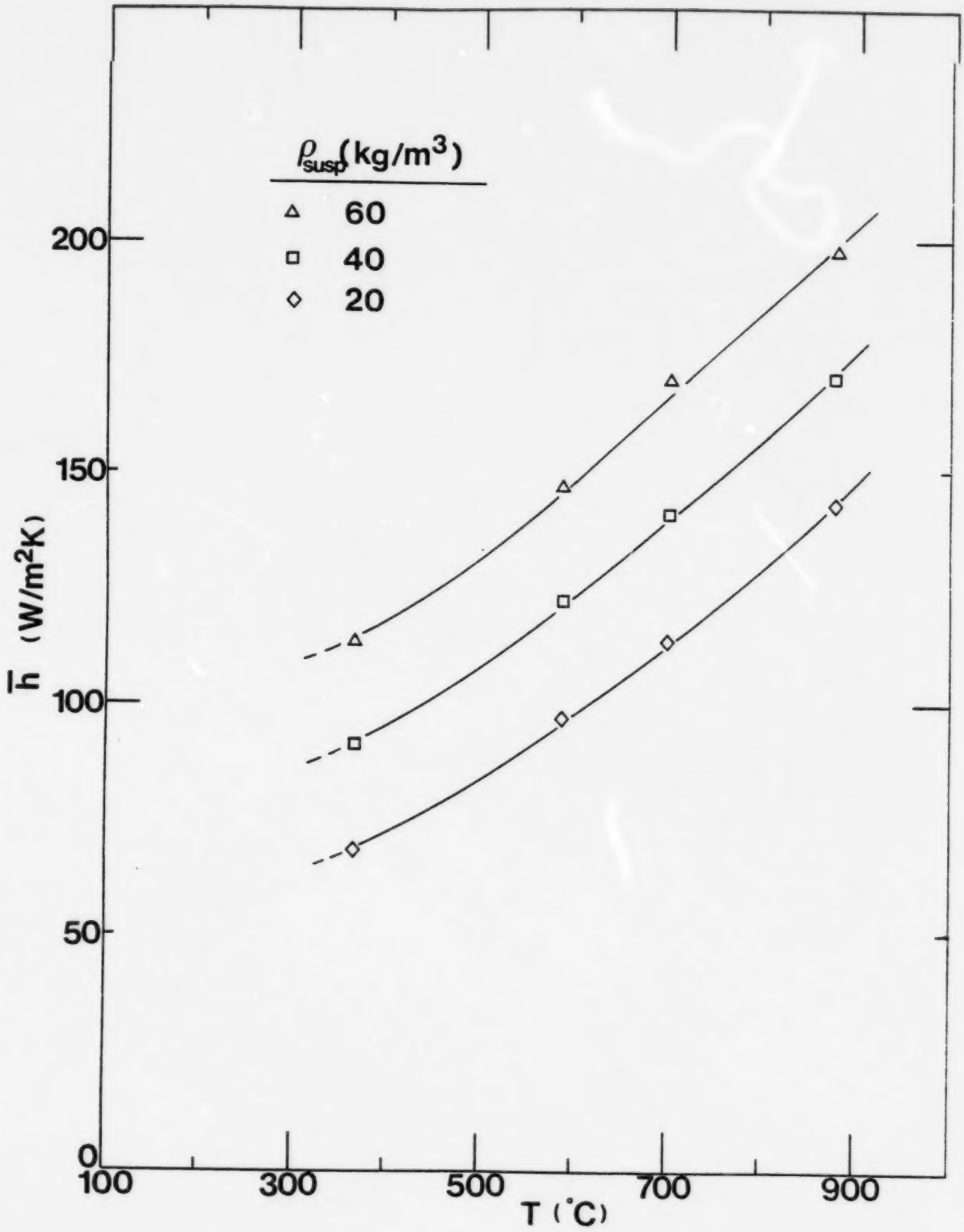

Figure 4.8: Crossplot of suspension to vertical tube heat transfer coefficient vs temperature for three suspension densities. Conditions as for Figure 4.7.

The influence of horizontal position is shown in Figure 4.9 where y represents the distance from the axis of the tube to the nearest wall of the vessel and Lo is the half-width of the column. For the highest temperature, 854 C, the heat transfer coefficient is highest for the tube at the centre of the column, with the value falling as the tube moves towards the wall and then increasing again when the tube comes very close to the wall, except for very low suspension densities. The lower set of four curves are for a lower temperature, 343 C. While the superficial velocity and particle size are also slightly different than for the upper set of four curves, these latter differences are too small to make a significant change. The difference between the two sets of curves is predominantly due to the temperature effect. At the lower temperature, the wall position leads to the highest coefficients over almost the entire range of suspension densities. These trends are probably due to the fact that most particles tend to be near the wall, leading to higher convective transfer in that region. Since this is the dominant mode of transfer at low temperatures, the maximum occurs at the wall. Because of shielding, radiation will tend to be less for a tube at or near the wall, and this accounts for the more complex curves at higher temperatures.

4.2 Temperature Profiles

A typical temperature profile for the facility running under combustion conditions appears in Figure 4.10. This profile was obtained with Highvale coal as the fuel during one of the preliminary runs when one of the membrane cooling surfaces was still present in the column. It is seen that there is some drop in temperature opposite the cooling surface, but that the temperature is quite uniform, within about a 50 C range around the entire loop. Once the membrane surface had been replaced by a single heat transfer tube (see section 2.5), temperature variations were even smaller, generally showing a maximum variation no larger than about 30 C around the entire loop. An exception to this, discussed in section 5.3 below, occurred in the woodwaste runs where larger temperature variations were recorded.

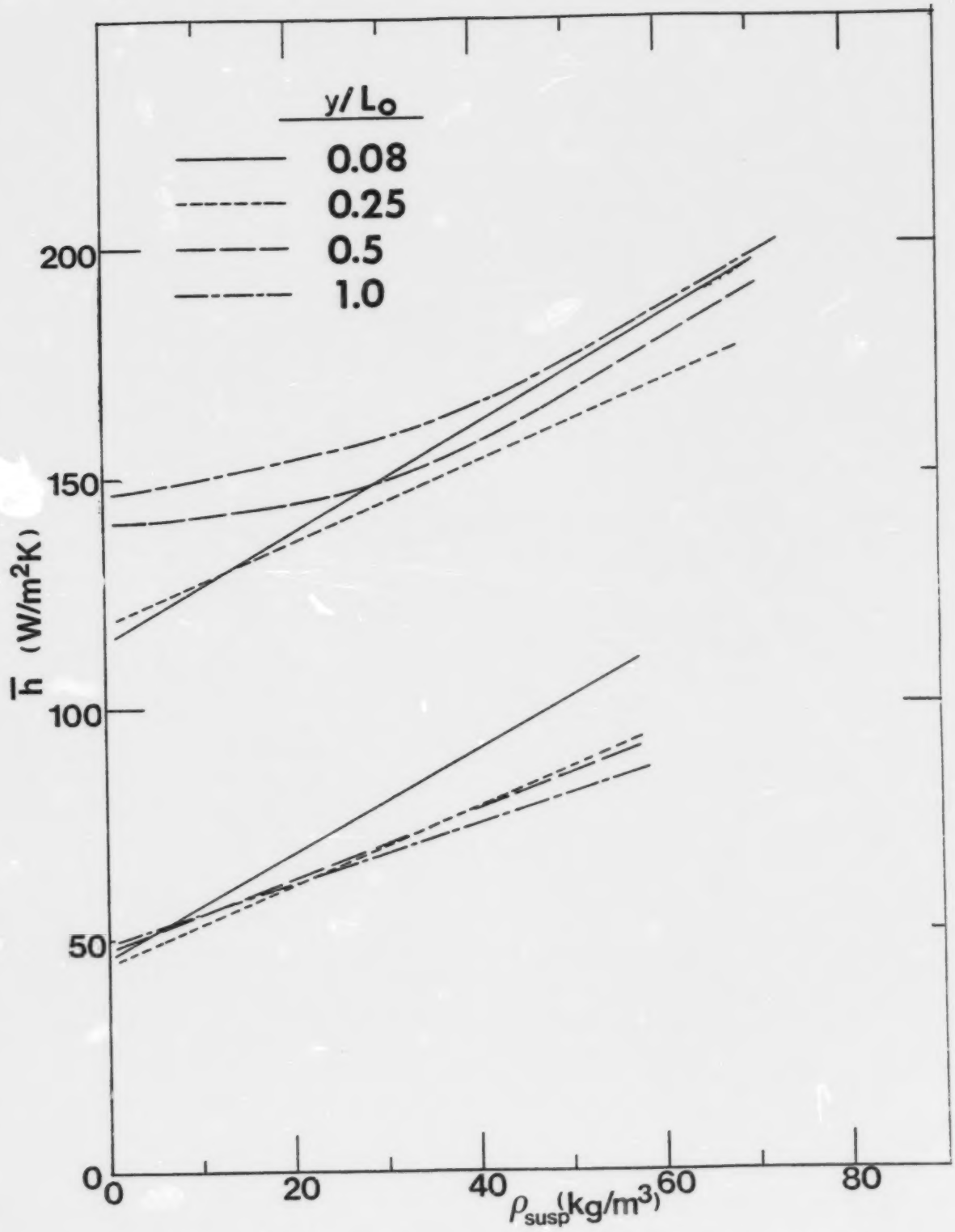

Figure 4.9: Suspension to vertical tube heat transfer coefficients for four different lateral distances between the axis of the tube and the wall. Upper four curves: T = 854 C; U = 8.5 m/s; dp = 227 um. Lower four curves: T = 343 C; U = 6.0 m/s; dp = 299 um.

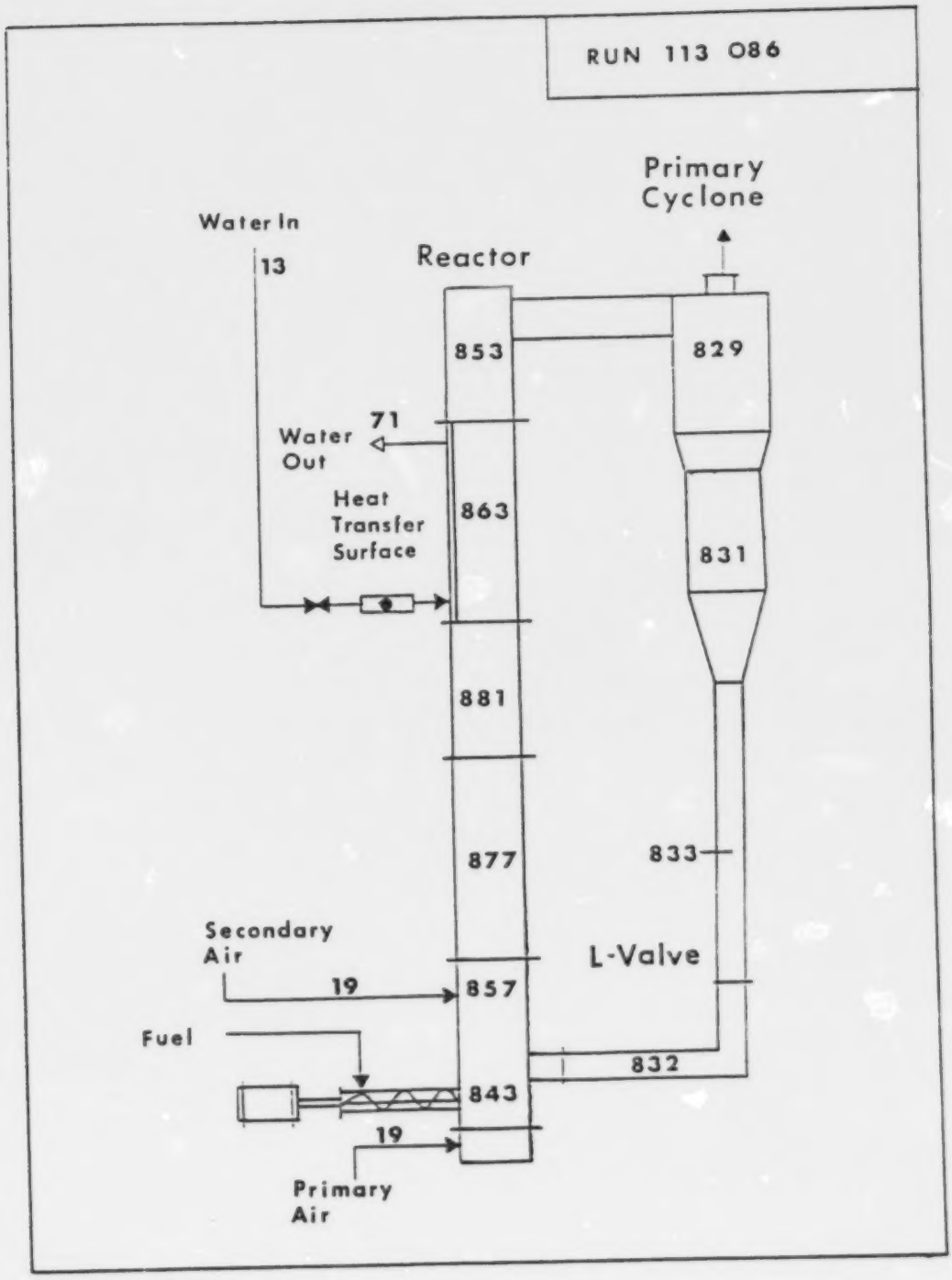

Figure 4.10: Typical temperature profile during combustion trial. Highvale coal; upper membrane cooling surface only in place.

5. COMBUSTION TESTS

5.1 Overview

A chronology of the various combustion runs conducted during the course of the contract is provided in Table 5.1. The duration of runs is the total time that the equipment was actually running, including start-up. The total duration of all tests, exclusive of the early heat transfer tests, adds up to 478 h. Some of the early runs were of a preliminary nature; detailed results for these tests are therefore omitted in this report. Likewise, there were a number of tests which had to be aborted due to malfunctions, feeding problems etc., and these are also generally excluded except where some useful results were obtained before the work had to be terminated.

5.2 Minto Coal Tests

Minto coal from New Brunswick is of special interest in Canada because it is the principal fuel in the new Chatham 22 MWe CFBC boiler. Earlier tests carried out for the Canadian Electrical Association (Dearborn, 1987) had indicated worrisome levels of calcium sulphide in the ash materials. CaS in the quantities measured (up to 6%) would cause serious leachate problems, making the ash unacceptable for landfill disposal. One of the objectives of our tests was therefore to generate solids waste samples which could be tested for CaS to see whether the concerns raised by the previous tests carried out in New Brunswick would be confirmed in our equipment. Elmtree limestone, also from New Brunswick and one of the sorbents to be tested at the Chatham plant, was chosen as the sorbent material.

The Minto coal is a high sulphur, highly agglomerating coal (see Tables 2.1 and 2.3 for properties.) The principal problem encountered with this coal in our equipment was sintering/agglomeration during the heat-up period. Measures taken to overcome this problem are detailed in section 3.3. Once the reactor had reached its full operating temperature (of the order of 870 C), a number of successful runs were completed. Conditions were chosen to simulate or bracket, as far as possible, those to be used in the Chatham unit and the range of conditions which are common in CFBC commercial operations.

A summary of some of the key findings is provided in Table 5.2. Sulphur capture and NOx emissions are also plotted in Figures 5.1 and 5.2, respectively. While it is impossible to keep all other conditions totally unchanged, it is seen that variations in temperatures, superficial gas velocities and secondary-to- primary air ratios are small. As expected, sulphur capture increased with increasing Ca:S

Table 5.1: Chronology of Combustion Runs

Mo/Yr	Fuel/Sorbent	Duration	Comments
10/86	Forestburg coal/None	14 h	Too much cooling surface
11/86	Forestburg coal/None	8 h	Sintering
11/86	Forestburg coal/Green Valley limestone	23 h	Some feeding problems; ran out of fuel
11/86	Esso coal/Green Valley limestone	42 h	Difficult start-up; low excess oxygen to reach 850C
12/86	Highvale coal/None; Hogfuel/None	22 h	Successful on coal; feeding problems with hogfuel
12/86	Pyrolysis char/Texlime	30 h	Fluctuating oxygen levels; high air flow required
01/87	Minto coal/Elmtree limestone	63 h	Ca:S=1.63 and 2.17; much improved control; low NOx; obtained ash samples
02/87	Minto coal/Elmtree limestone	44 h	Ca:S=2.72; ash samples; extra heat transfer data
02/87	Sawdust/None; Hogfuel/None	21 h	Start-up on natural gas and coal; successful operation on sawdust and hogfuel
03/87	Minto coal/Elmtree limestone	46 h	Ca:S=1.36; varied fraction secondary air, superficial velocity, circulation etc; extra heat transfer data
05/87	CANMET pitch/None	17 h	Tested pitch feeding system
06/87	CANMET pitch/Texlime	14 h	Water pressure problems, then feeding problems
06/87	CANMET pitch/Texlime	33 h	Agglomeration in bed; after clearing, hot spot led to emergency shutdown
06/87	CANMET pitch/Texlime	21 h	Pump failure
07/87	CANMET pitch/Texlime	30 h	Successful run
07/87	H-Oil pitch/Texlime	23 h	Building ventilation system failure
07/87	H-Oil pitch/Texlime	27 h	Some data; ventilation system again failed

Table 5.2: Test Results for Minto Coal/Elmtree Limestone for Different Calcium to Sulphur Ratios

Calcium to sulphur molar ratio	1.36	1.63	2.17	2.72
T in lower part of reactor, C	861	885	862	872
T in upper part of reactor, C	870	858	830	877
T at centre of L-valve, C	863	860	842	876
Sup. velocity below sec. air, m/s	3.3	3.4	3.2	3.6
Sup. velocity above sec. air, m/s	7.0	7.1	6.8	7.9
Secondary to primary air ratio	1.0	1.1	1.1	1.1
Coal feed rate, kg/h	19.1	18.4	18.8	21.5
Limestone feed rate, kg/h	5.8	6.7	9.2	13.1
Combustion efficiency, %	94	93	92	95
Oxygen in flue gas, %	2.0	3.4	3.4	3.5
SO2 in flue gas, p.p.m.	1836	1576	1205	770
Sulphur capture, %	72	74	80	88
Calcium utilization, %	53	45	37	33
NOx in flue gas, p.p.m.	130	113	134	149
CO in flue gas, p.p.m.	10-500	0-30	<20	0-20
Percent calcium sulphide sulphur:				
bed drain solids	*	0.22	0.21	0.23
L-valve solids	*	0.19	0.27	0.17
secondary cyclone catch	*	0.39	0.24	0.21
Mean particle diameter, um, for:				
bed drain solids	#	1770	2110	1340
L-valve solids	#	1450	1500	1310
secondary cyclone catch	32	32	25	34

* Values of 1.81, 1.33 and 0.50% were obtained for solids samples from the bed drain and secondary cyclone catch, respectively, at the end of the run. However, this run included a number of different operating conditions (see Table 5.3) with insufficient time for the solids to reach steady state composition for each set of conditions.

\# Runs were too short for steady state samples to be obtained.

Table 5.3 Effect of Operating Variable Changes on Emission Levels Minto Coal/Elmtree Limestone; Ca:S = 1.36

T in lower part of reactor, C	861	864	872	891	865	898
T in upper part of reactor, C	870	874	884	890	870	892
T at centre of L-valve, C	863	874	884	886	878	892
Sup. velocity above sec. air, m/s	7.0	8.1	7.9	7.6	9.8	10.8
Secondary/primary air ratio	1.0	1.5	1.4	0.42	1.5	1.4
Coal feed rate, kg/h	19.1	20.2	22.7	20.1	25.5	25.8
Overall suspension density, kg/m3	114	208	273	146	177	196
Oxygen in flue gas, %	2.0	3.0	3.2	3.5	3.7	3.4
Sulphur capture, %	72	70	71	69	67	67
NOx in flue gas, p.p.m.	130	138	136	145	146	140

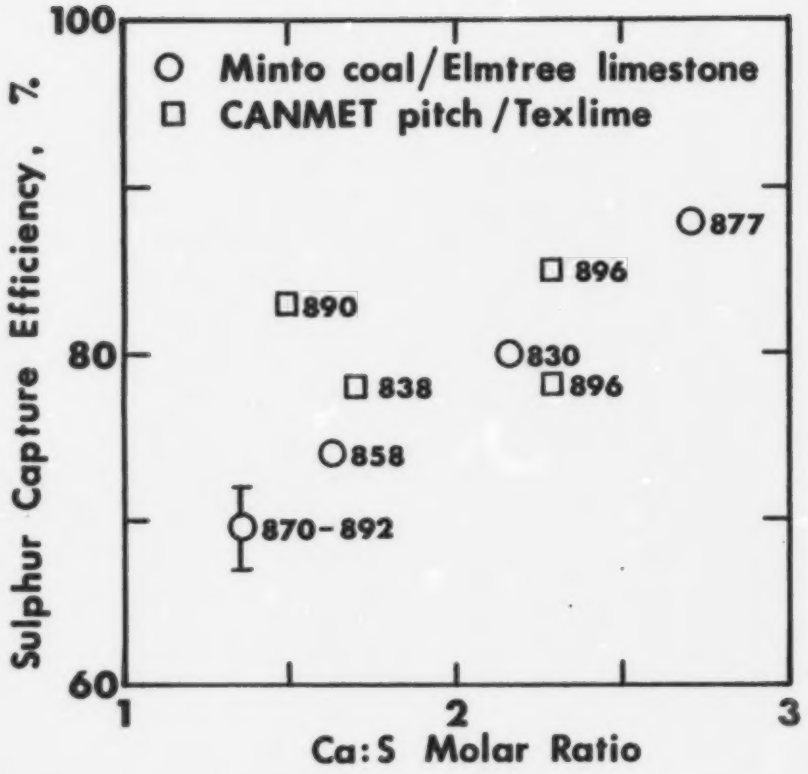

Figure 5.1: Sulphur capture versus Ca:S molar ratio for Minto coal and CANMET pitch tests.

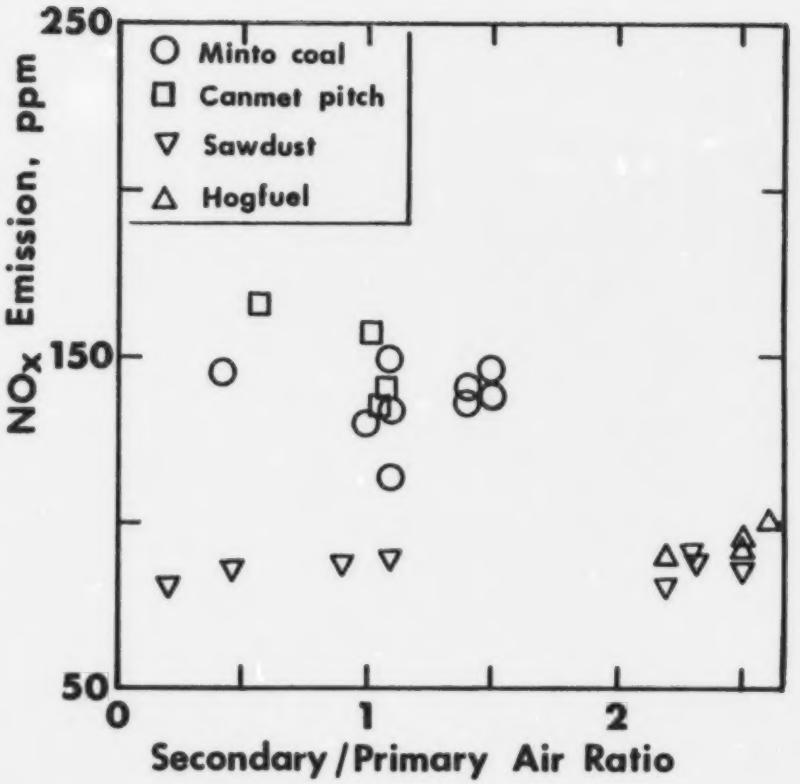

Figure 5.2: NOx emissions versus secondary/primary air ratio for four different fuels. Operating conditions are given in Tables 5.2 to 5.6.

ratio. This trend is also shown in Figure 5.1. While the overall sulphur capture is not as favourable as one might expect for CFBC units based on previous published results (e.g. Reh et al, 1980; Sahagian, 1984), it should be noted that the Elmtree limestone is not a particularly good sorbent (Becker and Code, 1983). In addition, better capture would be expected with a taller unit and with recycle of the fines captured in the secondary cyclone. While the addition of more limestone is seen to result in the capture of more sulphur, the calcium utilization (i.e. the fraction of the available calcium which is sulphated) is seen to decrease with increasing Ca:S ratio.

The other combustion indicators shown in Table 5.2 are seen to be relatively insensitive to the calcium to sulphur molar ratio. Combustion efficiencies (based on carbon conversion efficiencies) are in the range 92-95%. Again these values are somewhat lower than published CFBC values (e.g. Reh et al, 1980), and we would expect higher values for taller units and if the fines captured in the secondary cyclone were recycled to the combustion chamber. NOx levels are consistently below 150 p.p.m., well below existing environmental control limits. The CO concentration, determined by gas chromatography on syringe samples, varied widely, possibly due to uneven delivery of fuel by the screw feeder. As noted already in section 4.2, temperatures are seen to be very uniform, the maximum variation between any two thermocouples in the entire circulation loop generally not exceeding about 30 C.

Solids samples were obtained over prolonged periods of steady operation for the Ca:S molar ratios of 1.63, 2.17 and 2.72. Calcium sulphide levels obtained from the ash samples discharged from the bed drain valve, L-valve and secondary cyclone are tabulated in Table 5.2. The analyses were carried out by John Stephenson of Queen's University, and the results have been discussed elsewhere (Anthony, 1987). They show CaS levels consistently below 1% for the solids in our unit. Other properties of the solids samples relevant to disposal of CFBC wastes have been analysed by Dearborn Chemicals under a separate contract from the Government of Canada.

The cumulative particle size distributions of the samples are plotted in Figure 5.3. As expected, these show that the bed drain solids tend to be somewhat coarser than the solids sampled from the base of the L-valve, with the solids captured in the secondary cyclone being much finer than either of these.

Mean particle sizes are also given for the three solids streams in Table 5.2 with the Ca:S molar ratio held constant at 1.36. The mean sizes shown are Sauter mean diameters, determined by sieve analyses except in the case

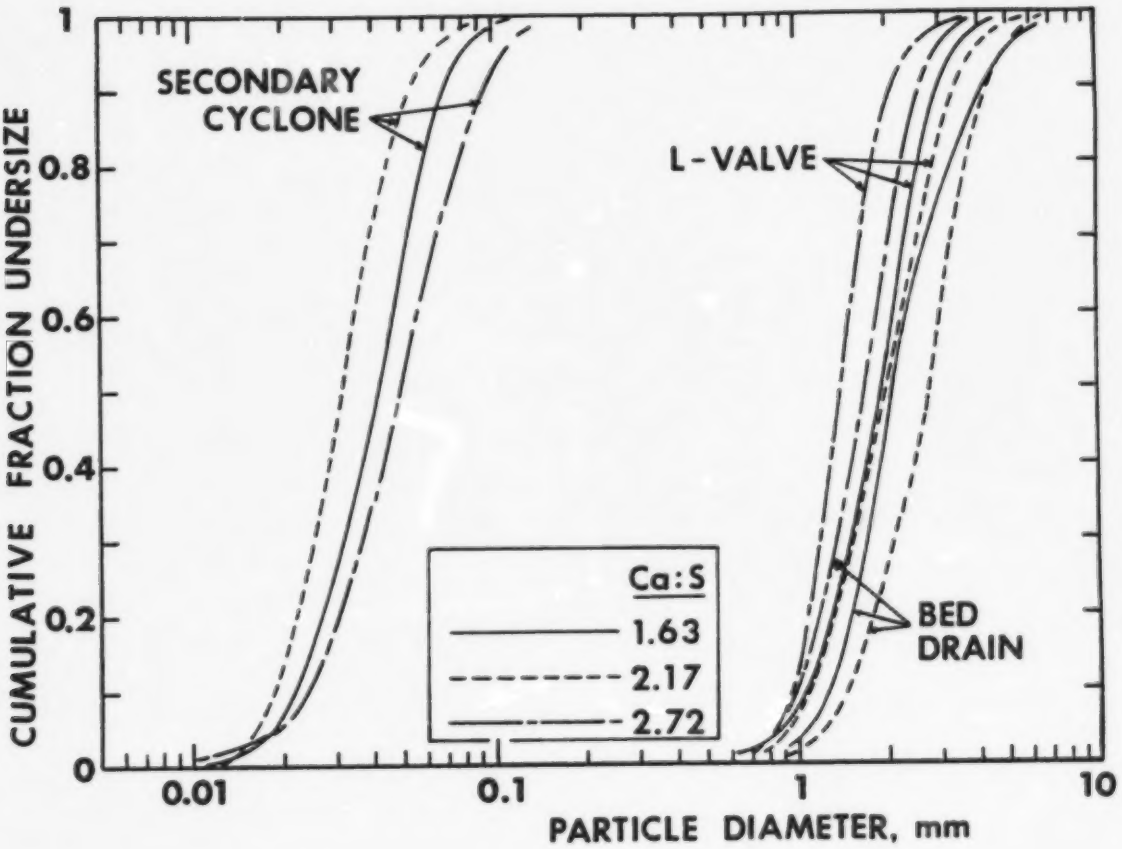

Figure 5.3: Particle size distributions for particulate materials withdrawn at the end of the Minto coal tests. For operating conditions see Table 5.2.

of the finest cyclone catch material which was analysed with a Coulter-type analyser. Once again, the bed drain material tends to be somewhat coarser than the L-valve solids, and both are much coarser than the material caught by the secondary cyclone.

The influence of changing a number of the operating variables is shown in Table 5.3. As far as possible, the temperatures and concentration of oxygen in the flue gas were kept constant while the solids circulation rate (and hence the overall suspension density), secondary/primary air ratio, and overall superficial velocity were varied within reasonable ranges. It is seen that sulphur capture is insensitive to changes in the suspension density and secondary/primary air ratio. A small drop in sulphur capture did occur when the superficial gas velocity was increased from 7-8 to 10-11 m/s. This probably results from the reduced residence time in the reactor and the increased carryover of fine fuel and sorbent particles at the higher superficial gas velocity. The NOx emissions appear to be insensitive to the changes in variables. While it is generally believed that secondary air is helpful in diminishing NOx levels, the influence here appears to have been small (see Figure 5.2). This result has also been noted in other CFBC studies (e.g. Ruottu et al, 1987). One possible explanation is that NOx levels may be controlled more by radial mixing than by staging.

5.3 Woodwaste Combustion Tests

Aside from the difficulty of maintaining steady and continuous feeding, woodwaste materials are relatively simple materials for circulating fluidized bed combustors. Since sulphur capture and solids waste composition were not of concern in this case, the runs were of shorter duration (see Table 5.1) Approximately 150 minutes was left between the end of the sawdust test and the beginning of data acquisition for the hogfuel for the system to re-establish steady conditions.

A typical temperature profile is shown in Figure 5.4, while temperature values for different secondary-to-primary air ratios and almost constant overall superficial gas velocity appear in Table 5.4. It was found that temperature profiles differed somewhat from the coal tests, with the temperatures tending to be higher at the top of the reactor and in the primary and secondary cyclone for both the sawdust and hogfuel than for the coals tested. This is no doubt due to the higher volatiles content and lighter particle density for the woodwaste materials, both factors promoting more burning in the upper section of the reactor and in the cyclones. A similar trend has been found by others (Stromberg, 1987) when burning woodwastes and peat.

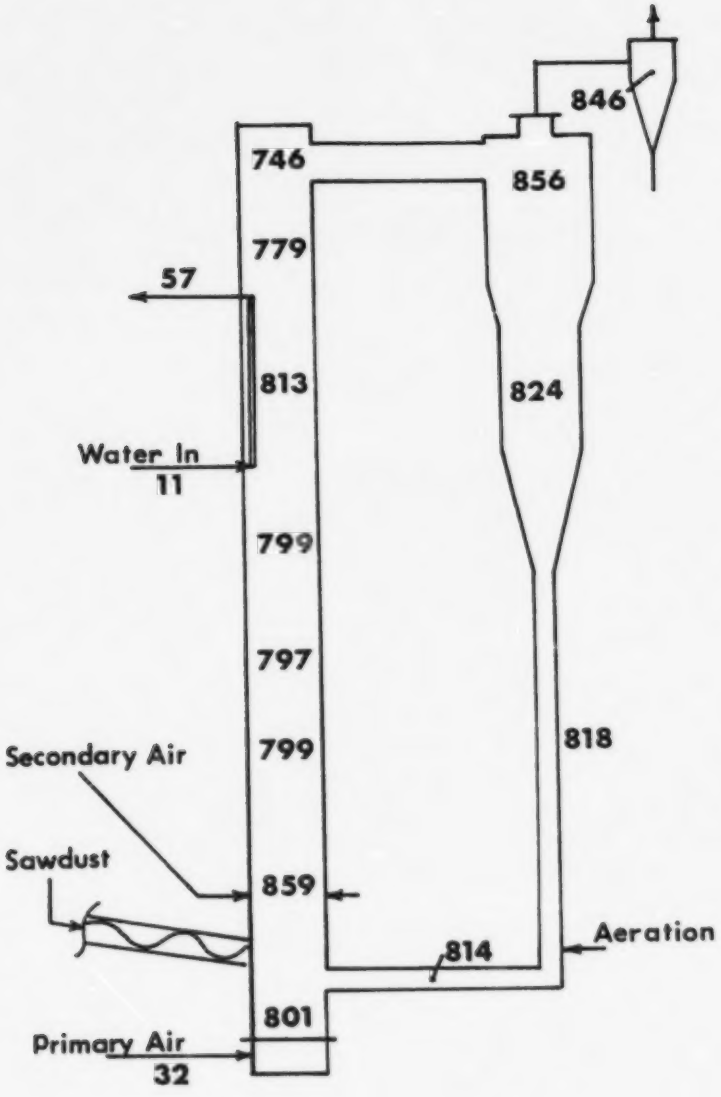

Figure 5.4: Instantaneous temperature profile during sawdust combustion trial.

Table 5.4: Superficial Gas Velocities, Secondary/ Primary Air Ratios, and Temperatures for Sawdust and Hogfuel Burning. For other conditions, see Table 5.5.

ID#	U(m/s)	Q2/Q1	Temperatures TR1	TR2	TC1	TC2	TS
	(a) Sawdust Combustion:						
80	7.4	2.2	860	826	856	815	834
84	7.3	2.3	836	819	852	814	826
86	8.0	2.5	854	819	848	768	824
90	8.3	2.4	868	818	845	790	824
94	7.6	1.1	863	812	856	854	824
97	7.1	0.91	878	800	845	838	808
	(b) Hogfuel Combustion:						
137	7.1	2.2	834	813	864	801	822
140	7.6	2.6	825	810	865	798	820
144	7.8	2.5	835	811	851	789	825
148	8.0	2.5	861	833	885	830	837
151	7.6	2.2	864	829	882	832	838
155	7.6	0.73	921	821	878	837	831
159	7.3	0.21	969	837	876	825	825

Table 5.5: Gaseous Emissions and Suspension Densities for Sawdust and Hogfuel Burning. See Table 5.4 for other conditions.

ID#	Av.Susp. Density (kg/m3)	Measured Flue Gas Concentrations Oxygen (%)	NOx (ppm)	CO2 (%)	CO (ppm)
	(a) Sawdust Combustion:				
80	123	2.1	80	-	-
84	111	2.4	88	17.9	240
86	113	4.1	85	16.5	1680
90	128	5.3	85	17.3	370
94	129	3.4	88	18.4	1060
97	166	4.4	87	18.0	1590
	(b) Hogfuel Combustion:				
137	119	3.0	89	-	-
140	80	4.5	100	17.6	28
144	115	4.1	95	18.2	710
148	113	2.3	94	18.3	377
151	104	2.6	90	18.3	<10
155	82	3.5	85	19.2	640
159	58	3.2	80	-	-

Some measured flue gas concentrations are given in Table 5.5. The measured NOx concentrations are also plotted in Figure 5.2. Concentrations of NOx are seen to be low, always 100 p.p.m. or less. They are no doubt smaller than for coal and pitch because the fuel nitrogen levels are lower (see Table 5.1). The measured CO levels, determined by gas chromography on syringe samples, were found to be highly variable and are generally much higher than desirable. We believe that the variations result from fluctuations in the feed rate of the woodwastes, probably originating from the screw feeder which turns at a speed of the order of 10 r.p.m. and which probably delivers the waste material in slugs rather than as a continuous stream. There were indications of high molecular weight hydrocarbons, possibly phenolic in nature, but these could not be fully characterized in the gas chromatograph employed for analysis. The high magnitude of the CO concentrations could no doubt be lowered substantially by using a taller reactor or by decreasing the superficial gas velocity to give longer residence time in the combustion chamber. In the current work the reactor height was limited by the height of the laboratory, while the superficial velocity could not be decreased below about 7 m/s without a significant drop in temperature. It is notable that the heavier hogfuel particles gave lower CO levels than the sawdust, the latter being more readily entrained. In applications of circulating fluidized beds, it is clearly important to assure that as much heat release as possible take place within the combustion chamber.

5.4 Pitch Combustion Tests

Pitch materials (also sometimes referred to as tars) constitute the bottoms fractions or residue from efforts to upgrade unconventional crude hydrocarbons like heavy oils and tar sands bitumen. These materials, here simply referred to as "pitch", tend to be high in asphaltenes and other high molecular weight hydocarbons, often aromatic in nature. They also tend to be high in sulphur, and to be the repository of most of the heavy metals which naturally occur in small quantities of the original hydrocarbon material.

These pitch materials represent a potentially troublesome byproduct of upgrading operations for unconventional feedstocks and fuels in Canada and in other countries. It would be very useful if a means could be found of safely disposing of the pitch fraction, especially if this could be accomplished with recovery of energy. Circulating fluidized bed combustion represents one possible means of incinerating pitch materials with simultaneous capture of the sulphur in a suitable sorbent and trapping of the heavy metals in a solids residue which is much smaller in volume than the original pitch material.

Key properties of the two pitches used in our tests are listed in Tables 2.2 and 2.5. The sorbent employed in these tests was Texlime from Texada Lime in Langley, B.C. Its key properties are given in Tables 2.3 and 2.4.

5.4.1 CANMET pitch combustion trials

The first pitch tested was obtained from the 524 C+ residual fraction produced by the CANMET Hydrocracking Demonstration Unit in the Petro-Canada Montreal East refinery. This process uses an additive to inhibit coke formation while converting high boiling hydrocarbons into light products (Paquette et al, 1987). The process was originally developed at CANMET (Pruden, 1978) to upgrade oil sands bitumen and heavy oils of Canadian origin, and has subsequently been extended to the processing of the bottom of the barrel from conventional crudes.

The principal problems encountered in testing this fuel were in feeding it continuously into the reactor and in preventing it from leading to defluidized regions within the reactor. The means of preventing these problems have already been discussed in section 3.3. In brief, successful feeding was achieved by melting the pitch and maintaining a temperature of 190 C or higher throughout the entire feed piping and nozzle system. Success in maintaining combustion inside the reactor depended on achieving good atomization in the injection nozzle and on having the bed sufficiently hot (at least 750 C) before commencing pitch feeding. The latter was accomplished by starting up the unit with Highvale coal and then switching over to the pitch once the minimum temperature had been achieved. With these precautions and measures, developed largely as result of empirical trial and error, the test run proceeded smoothly, the liquid pitch providing a more uniform feed than any of the solids fed in our trials. The pitch also appeared to be quite reactive.

The principal results are shown in Table 5.6. The sulphur capture and NOx emission levels are also plotted in Figures 5.1 and 5.2, respectively. The equipment was operated at two different superficial gas velocity levels (about 7.6 m/s and 5.6 m/s), at two different secondary/primary air ratios (0.56 and about 1.05), and at Ca:S molar ratios from 1.5 and 2.3). The outlet oxygen concentration was maintained in the 3-4% range and, except for Condition 1 where the temperature was about 850 C, the temperature was maintained close to 900 C. The solids circulation flux, and hence the mean suspension density, were varied in such a manner that the temperature could be maintained.

Table 5.6: Summary of Combustion Results for CANMET Pitch

Condition	1	2	3	4
Superficial Velocity below Sec. Air, m/s	4.6	3.6	3.4	2.7
Superficial Velocity above Sec. Air, m/s	7.5	7.8	7.5	5.6
Secondary to Primary Air Ratio	0.56	1.07	1.05	1.03
Pitch Feedrate, kg/h	15.6	15.8	15.5	11.1
Limestone Feedrate, kg/h	2.3	2.1	3.2	2.3
Ca:S Molar Ratio	1.7	1.5	2.3	2.3
Excess Air, %	18	16	13	18
Solids Circulation Rate, kg/m2s	33	30	38	22
Average Suspension Density, kg/m3	75	81	104	52
Temperature at Bottom of Reactor, C	855	899	906	913
Temperature at Top of Reactor, C	838	890	896	896
Temperature at Centre of L-valve, C	836	877	887	874
Temperature in Secondary Cyclone, C	881	863	871	856
Oxygen Concentration in Flue Gas, %	3.8	3.4	3.0	3.8
SO2 Concentration in Flue Gas. ppm	382	291	404	254
NOx Concentration in Flue Gas, ppm	165	140	135	157
CO Concentration in Flue Gas, ppm	N.D.	400-800	300-1000	500-700
Sulphur Capture, %	78	83	78	85
Calcium Utilization, %	47	56	33	37
Combustion Efficiency*, %	91	99	98	99
Mean Particle Size of Bed Drain Material, um	348	355	351	308
Mean Particle Size of L-valve Material, um	328	329	343	307
Mean Particle Size of 2ndy. Cyclone Material, um	29	48	30	32
Percent CaS Sulphur for:				
Bed Drain Solids	0.02	0.05	0.04	0.00
L-Valve Solids	0.01	0.03	0.05	0.05
2ndy. Cyclone Catch	0.02	0.35	0.12	0.02

* Combustion efficiency determined as carbon conversion efficiency.

The relatively high temperatures in the secondary cyclone suggest that some combustion was occurring in the primary and secondary cyclones. As shown in Figure 5.1, sulphur capture was somewhat better than in the Minto coal tests and showed remarkably little influence of the Ca:S ratio over the range studied. Except for the first condition where the temperature was significantly lower and where there were some difficulties with blockage in the secondary cyclone standpipe which may have affected the composition of the solids sampled there, the combustion efficiency was favourable. This suggests that the combustion temperature should be maintained at about 890 C or higher to assure good burn-up. The few measurements of CO concentration obtained by gas chromatography appear to be higher than desirable; further study is needed using a continuous on-line analyser.

NOx levels were surprisingly a little higher for the lower temperature, but values were in a rather narrow range, from 135 to 165 p.p.m., well within existing environmental limits. As shown in Figure 5.2, NOx levels were found to be somewhat higher for the pitch than for the Minto coal trials and considerably higher than for the woodwaste runs, reflecting the relative nitrogen contents of the different fuels (see Tables 2.1 and 2.2). The mean particle size of solids samples withdrawn from the bed drain and L-valve outlet were consistently in the 300-360 um range, while the material collected in the secondary cyclone was much finer, always less than 50 um on average.

The metals contents of the solids samples are shown in Table 5.7. The LOF values represent "loss on firing" into the atomic absorption inductively coupled plasma (ICP) analyser and may signify carbon or uncalcined limestone. The original make-up of the pitch, olivine sand and limestone are given in Tables 2.5 and 2.4. The high levels of magnesium oxide in the different samples results primarily from its presence in the olivine sand.

Of special interest in Table 5.7 are the amounts of vanadium and nickel in the different waste streams. These materials are highly corrosive and somewhat toxic. It is therefore desirable that they remain in the solid residue, and this has been largely found to be the case with atmospheric bubbling fluidized bed combustion trials (Becker et al, 1985) and with CFBC trials (Polymath et al, 1986; Hamer et al, 1987) for two particulate fuels, Syncrude coke and Minto coal. However, the results shown in Table 5.7 indicate possible escape of the vanadium in our facility with liquid pitch feed, since the vanadium content of the original pitch ash is three times that of the nickel, but reports at a much lower concentration in each of the solids samples analysed. It should be noted, however, that the vanadium principally ended up in the finest baghouse stream

Table 5.7: Metals Content in Solids Samples from CANMET Pitch Trial
All numbers are percents by weight determined by ICP Atomic Absorption.

	Condition 1*			Condition 2*			Condition 3*			Condition 4		
	Bed Drain	L-Valve	Sec. Cycl.	Bed Drain	L-Valve	Sec. Cycl.	Bed Drain	L-Valve	Sec. Cycl.	Bed Drain	L-Valve	Sec. Cycl.
SiO_2	40.64	42.57	25.46	40.64	39.23	31.66	40.64	40.33	25.30	40.66	40.76	28.67
Al_2O_3	1.04	0.49	7.46	0.45	0.40	2.03	0.38	0.42	1.40	1.70	0.93	2.08
Fe_2O_3	8.29	8.58	2.85	8.58	8.70	6.79	8.92	8.66	6.12	8.31	8.63	6.72
TiO_2	0.03	0.02	0.21	0.03	0.02	0.07	0.03	0.02	0.07	0.04	0.03	0.08
P_2O_5	0.06	0.07	0.00	0.09	0.07	0.00	0.09	0.06	0.00	0.04	0.03	0.00
CaO	3.95	3.97	6.22	3.87	4.45	15.94	3.82	4.19	29.04	4.55	4.18	25.19
MgO	42.94	43.11	9.32	43.27	43.32	27.31	43.34	43.93	21.75	41.70	43.65	25.62
SO_3	0.48	0.42	0.03	0.71	0.52	1.77	0.73	0.69	3.31	0.85	0.77	4.26
Na_2O	0.07	0.06	0.44	0.05	0.05	0.13	0.06	0.06	0.12	0.11	0.08	0.14
K_2O	0.06	0.03	0.14	0.02	0.04	0.12	0.03	0.05	0.14	0.10	0.09	0.16
BaO	0.03	0.03	0.10	0.03	0.03	0.04	0.03	0.03	0.04	0.03	0.03	0.04
SrO	0.01	0.01	0.03	0.01	0.01	0.03	0.01	0.01	0.06	0.02	0.02	0.05
V_2O_5	0.02	0.02	0.00	0.04	0.03	0.10	0.05	0.04	0.12	0.05	0.06	0.16
NiO	0.34	0.33	0.06	0.33	0.34	0.25	0.34	0.34	0.26	0.33	0.61	0.27
LOF	0.00	0.00	45.51	0.00	1.09	12.08	0.00	0.00	11.54	0.40	0.00	4.46
Sum	97.96	99.71	97.83	98.12	98.30	98.32	98.47	98.83	99.24	98.89	99.87	97.90
Carbon	0.43	0.14	38.21	0.13	0.15	7.50	0.09	0.12	5.33	0.10	0.11	1.45

* See Table 5.6 for details of each of the four operating conditions.
Note: MnO_2, Co_3O_4, MoO_3, SnO_2, ZnO and CuO were less than 0.01% in all samples and have not been included in the table.

in the earlier trials (Becker et al, 1985; Polymath et al, 1986; Hamer et al, 1987) and that our baghouse had not yet been installed when the trials reported here were conducted. In addition, it is possible for heavy metals to adsorb onto refractory surfaces, so that very long trials may be needed to obtain an accurate picture of where the vanadium is going. Hence the low apparent vanadium values do not necessarily mean discharge in vapour form, but further tests are certainly needed to resolve this issue.

5.4.2 AOSTRA H-Oil pitch combustion trials

The Alberta Oil Sands Technology and Research Authority (AOSTRA) has been promoting the development of upgrading technology for a number of years. Tests have been conducted using a variety of upgrading processes developed in a number of countries to determine which can best meet the needs of oil sands bitumen. The second pitch tested was a byproduct of one such test, carried out in New Jersey on Cold Lake vacuum bottoms with the H-Oil Process developed by Hydrocarbon Research Incorporated.

The trials on the H-Oil pitch were largely unsuccessful due to problems with the building ventilation system. The fragmentary results which were obtained are summarized in Table 5.8. These indicate a good combustion efficiency, low NOx emissions and favourable calcium utilization for the limited range of conditions investigated. An observation in this run was that the combustion appeared to generate a significant cloud of fine fly ash, not present for any of the other fuels tested. This may have contributed to the ventilation problems which led to termination of the trials on two separate occasions. Clearly, more trials are needed with this fuel with the baghouse in place in order to fully test this fuel. A further test is planned in the next stage of this work.

Table 5.8: Summary of Results for AOSTRA H-Oil Pitch

Condition	1	2	3
Superficial velocity below secondary air inlet, m/s	4.6	4.9	5.1
Superficial velocity above secondary air	7.0	7.8	8.2
Secondary/primary air ratio	0.52	0.57	0.58
Pitch feedrate, kg/h	14.6	15.1	14.9
Limestone feedrate, kg/h	0.60	0.78	1.35
Ca:S molar ratio	0.54	0.68	1.2
Solids circulation flux, kg/m2h	55	79	N.A.
Average suspension density, kg/m3	65	97	N.A.
Temperature at bottom of reactor, C	872	826	897
Temperature at top of reactor, C	837	818	891
Temperature at centre of L-valve standpipe, C	818	828	865
Temperature in secondary cyclone, C	787	809	746
Oxygen concentration in flue gas, %	2.4	3.7	3.6
SO2 concentration in flue gas, ppm	845	677	204
NOx concentration in flue gas, ppm	105	125	100
Sulphur capture, %	44	55	87
Calcium utilization, %	82	81	72
Combustion efficiency, %	98-99	N.A.	N.A.

Notes: 1) N.A. means not available.
2) Sorbent was Texlime supplied by Texada Lime, Langley.
3) Ventilation problems led to premature termination of the test run with incomplete results.

6. CONCLUSIONS AND RECOMMENDATIONS

6.1 Conclusions

A pilot plant scale, high temperature circulating fluidized bed facility was modified to allow it to be used for continuous combustion testing by adding feeding systems for particulate solid fuels, liquid fuels and limestone sorbents. Analytical instrumentation and data acquisition capability were also added during the course of the contract. The membrane heat transfer surfaces were replaced for most of the tests by a single vertical cooling tube which could be used for measuring suspension-to-surface heat transfer coefficients over a broad range of temperatures.

It has been shown that circulating fluidized bed combustion is capable of burning difficult fuels such as a high sulphur, agglomerating (Minto) coal, hogfuel, and pitch derived from upgrading of unconventional crude hydrocarbons. Achieving continuous and uniform feeding and maintaining the combustion temperature above a minimum temperature which depends on the fuel were found to be essential to the successful operation of the facility for these fuels. In total, 478 hours of operation under combustion conditions were completed during the course of the 16-month contract.

In general, the tests resulted in low emissions of NOx, good capture of sulphur and good combustion efficiencies. NOx levels ranged from 80-100 ppm for the woodwaste materials to 140-165 ppm for one of the pitches, and tended to be rather insensitive to the operating conditions for a given fuel. Sulphur capture increased and calcium utilization decreased with increasing Ca:S molar ratio. Calcium sulphide levels in solids samples were consistently less than 1% by weight for all the samples analysed. However, there were indications that a significant proportion of the vanadium contained in one of the original pitch materials tested did not end up in the solids waste materials. As expected, the solids withdrawn from the bottom of the reactor tended to be somewhat coarser than those discharged from a valve at the apex of the L-valve. Both of these streams were much coarser than the solids capture by the secondary cyclone. The latter were also much richer in carbon and in sulphated limestone than the bed and L-valve solids.

Temperature profiles measured around the circuit of the circulating bed showed relatively little variation from position to position. Suspension to surface heat transfer coefficients were shown to depend strongly on the local cross-sectional suspension density, but to be insensitive to the superficial gas velocity at a constant

suspension density. Heater length was found to be an important factor in determining heat transfer coefficients, longer surfaces showing lower transfer and less particle size dependence than miniature heat transfer surfaces. Radiation plays an important role in determining heat transfer coefficients at combustion temperatures, contributing of the order of 60-80 W/m2K of the total coefficients which are typically of order 100-200 W/m2K for the long surfaces examined in this work. The lateral position of a vertical cooling tube was also found to have some influence on the heat transfer coefficient.

6.2 Recommendations

Several equipment modifications should be made before further tests are carried out:

(a) The baghouse must be installed to permit sampling of the finest solids emitted and to reduce the load on the building ventilation system.

(b) Provision should be made for returning solids captured in the secondary cyclone to the bottom of the riser section. It is anticipated that this will improve both the combustion efficiency and the sulphur capture of the system. To reduce blockage problems in the standpipe from the secondary cyclone, the standpipe diameter should be enlarged.

(c) In order to reduce problems of agglomeration and sintering, the bottom section of the reactor should be tapered to increase the superficial velocity of the gas at the bottom of the riser. Provision should also be made for discharging agglomerates or oversized solids directly downwards through the distributor plate.

(d) Steps should be taken to eliminate as much heat loss as possible in order that the controllable heat removal be as large a fraction as possible of the overall heat release. This would permit the unit to be operated over a broader range of operating conditions and should allow one of the membrane surfaces to be reinstated.

(e) It would be helpful if analysers could be installed for continuous on-line measurements of the concentrations of CO, CO2 and unburnt hydrocarbons in the flue gas.

(f) Output from the gas analysers and from pressure transducers purchased but not installed under the contract should be recorded on the computer data acquisition system.

(g) The small offset in the standpipe of the L-valve appears to cause the solids return to be less steady than one would wish. The standpipe should be modified to make it totally vertical as well as to reduce heat losses from this part of the system.

(h) Provision should be made for multi-point sampling of gases and solids to assist in developing steady state and dynamic models for the CFBC system.

(i) Shields should be provided to extend the lifetime of the thermocouples used in the reactor chamber.

Several tests should be completed or extended to answer questions raised by this work. A further attempt should be made to burn the H-Oil pitch, since trials with this fuel were only partially successful. Longer tests under steady state conditions and with the baghouse in place should be carried out also with CANMET pitch in order to assess the whereabouts of the vanadium which enters with the fuel. It would also be helpful to have baghouse samples for one of the Minto coal conditions to compare with previous results for calcium sulphide and to permit work to be extended on the disposal characteristics of solid waste materials. This would also allow the influence of secondary cyclone recycle to be evaluated.

Among the further work which would be useful to do using the U.B.C. pilot scale circulating bed combustion facility are the following:

(a) The equipment would lend itself well to a study which would seek to identify changes in the compositions of solids and gas with position. This would be very helpful in understanding the processes which govern the generation and oxidation of calcium sulphide, the production and reduction of nitrogen oxides, limestone sulphation and heat release. The results would also be very helpful in testing models for circulating fluidized bed combustion.

(b) The unit would be useful for studying the combustion of additional fuels, e.g. black liquor, refuse-derived fuels or organic waste liquids, not previously tested in CFBC units.

(c) In order to compare the extensive hydrodynamic results obtained in our laboratory under cold modelling conditions, a high temperature capacitance or optical probe should be tested at combustion temperatures in the pilot CFBC unit.

(d) Additional heat transfer results should be obtained with the membrane cooling surfaces in place at combustion temperatures.

NOMENCLATURE

dp	mean particle diameter
h	suspension to surface heat transfer coefficient
Lo	half column width
Q1	primary air flow rate to base of the column
Q2	secondary air flow rate to the column
T	temperature
TR1	temperature in the lower part of the reactor
TR2	temperature in the upper part of the reactor
TC1	temperature in the primary cyclone
TC2	temperature in the secondary cyclone
TS	temperature in the standpipe of the L-valve
U	superficial gas velocity
y	distance from tube axis to nearest column wall
susp	cross-sectional mean suspension density

REFERENCES

Anthony, E.J., J.R. Stephenson and A.P. de Iribarne, Calcium sulphide formation in solid wastes from circulating fluidized bed combustors, Paper presented at 9th International Fluidized Bed Combustion Conference, Boston, May, 1987.

Becker, H.A. and R.K. Code, Pilot plant trials on atmospheric fluidized bed combustion of high-sulphur Eastern Canadian coals (Minto and Devco) with limestone addition for sulphur capture, Tech. Rept. QFBC.TR.83.1, Queen's University, Kingston, Ontario, 1983.

Becker, H.A., R.K. Code, R. McCleave and J.R. Stephenson, Pilot plant studies of fluidized coal combustion, Tech. Rept. QFBC.TR.85.1, Queen's University, Kingston, Ontario, 1985.

Brereton, C.M.H., Fluid mechanics of high velocity fluidised beds, Ph.D. dissertation, University of British Columbia, 1987.

Burkell, J.J., Solids circulation rate measurement in a circulating fluidized bed, M.A.Sc. dissertation, University of British Columbia, 1986.

Burkell, J.J., J.R. Grace, J. Zhao and C.J. Lim, Measurement of solids circulation rates in circulating fluidized beds, 2nd Intern. Conf. on Circulating Fluidized Beds, Compiegne, France, March, 1988.

Couturier, M.F., Sulphur dioxide removal in fluidized bed combustors, Tech. Rept. QFBC.TR.86.1, Queen's University, Kingston, Ontario, 1986.

Dearborn Environmental Consulting Group, Characterization of circulating bed AFBC wastes, Rept. for the Canadian Electrical Association, October, 1986.

Dearborn Environmental Consulting Group, Technical Options for the disposal of CFBC solid wastes, DSS File No. 52SS.KE 145-6-0643, 1988.

Geldart, D., Types of gas fluidization, Powder Technol., 7, 285-292(1973).

Glicksman, L.R., Circulating fluidized bed heat transfer, 2nd Intern. Conf. on Circulating Fluidized Beds, Compiegne, France, March, 1988.

Grace, J.R., Heat transfer in circulating beds, in Circulating Fluidized Bed Technology, ed. P. Basu, Pergamon Press, Toronto, pp. 63-80, 1986a.

Grace, J.R., Contacting modes and behaviour classification of gas-solid and other two-phase suspensions, Can.J.Chem. Eng., 64, 353-363(1986b).

Grace, J.R., C.J. Lim, C.M.H. Brereton and J. Chaouki, Circulating fluidized bed reactor design and operation, Sadhana, 10, 35-48(1987).

Hakansson, K., Development of an oxygen probe for a circulating fluidized bed combustor, B.A.Sc. thesis, University of British Columbia, Dept. of Chemical Engineering, 1987.

Hamer, C.A., D.T. Liang and J.B. Kearns, Combustion trials with Syncrude coke and Minto coal in the Mineral Sciences Laboratories circulating fluidized bed combustor: sulphur and metals capture and metallic corrosion, Rept. MSL 87-92, July, 1987.

Knowlton, T.M. and I. Hirsan, L-valve characterized for solids flow, Hydrocarb. Proc., No. 3, 149-153(1978).

Paquette, J.P., A.E. Silva and G. Muir, CANMET Hydrocracking Process demonstration plant - operating experience, 37th Can. Chem. Eng. Conf., Montreal, May, 1987.

Polymath Energy Consultants Ltd., Ahlstrom Corporation and Pyropower Corporation, Combustion, sulphur neutralisation and vanadium balance tests with Syncrude coke and Fort McMurray limestone in a pilot-scale atmospheric recirculating fluidised-bed reactor, Final Rept. on DSS Contract No. 23SQ.23440-4-9239, July, 1986.

Pruden, B.B., Hydrocracking of bitumen and heavy oils at CANMET, Can. J. Chem. Eng., 56, 277-280(1978).

Reh, L., H-W. Schmidt, G. Daradimos and V. Petersen, Circulating fluidbed combustion, an efficient technology for energy supply and environmental protection, Proc. Inst. Energy International Conference, paper VI-2, 1980.

Ruottu, S., P. Sarkomaa and R. Tammilehto, Development of a CFB reactor with a horizontal cyclone, Paper presented at 9th International Fluidized Bed Combustion Conference, Boston, May, 1987.

Sahagian, J., Commercial development of fluidized beds for direct combustion of tar sands and other oil bearing materials, Energy Progress, 4, 51-53(1984).

Stromberg, L., Studsvik Energiteknik, Nykoping, Sweden, Personal Communication, 1987.

Tibbetts, T.E. and W.J. Montgomery, Evaluation of Canadian commercial coals, Canmet Rept. 76-40, Energy Research Laboratories, CANMET, Energy Mines and Resources Canada, 1976.

Wu, R.L., C.J. Lim, J. Chaouki and J.R. Grace, Heat transfer from a circulating fluidized bed to membrane waterwall surfaces, A.I.Ch.E. Journal, 33, 1888-1893(1987).